(4)

TECHNICAL REPORT BRL-TR-3059

BRL

CALCULATED GUN INTERIOR BALLISTIC EFFECTS OF IN-DEPTH BURNING OF VHBR PROPELLANT

FREDERICK W. ROBBINS
DAVID L. KRUCZYNSKI

NOVEMBER 1989

U.S. ARMY LABORATORY COMMAND

BALLISTIC RESEARCH LABORATORY
ABERDEEN PROVING GROUND, MARYLAND

DISCLAIMER NOTICE

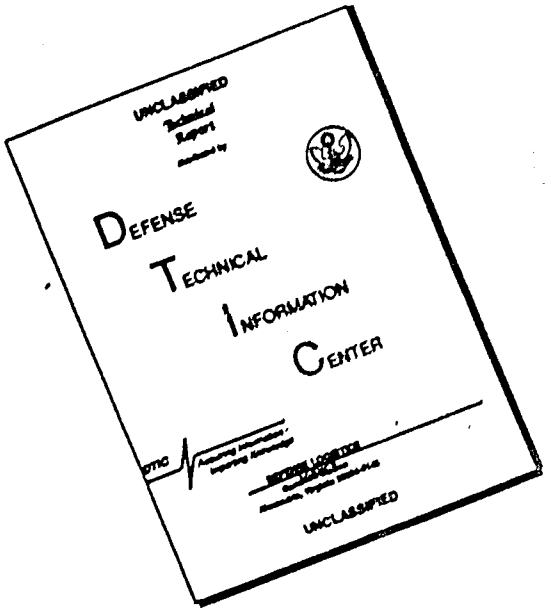

THIS DOCUMENT IS BEST QUALITY AVAILABLE. THE COPY FURNISHED TO DTIC CONTAINED A SIGNIFICANT NUMBER OF PAGES WHICH DO NOT REPRODUCE LEGIBLY.

UNCLASSIFIED
SECURITY CLASSIFICATION OF THIS PAGE

REPORT DOCUMENTATION PAGE

Form Approved OMB No. 0704-0188

1a REPORT SECURITY CLASSIFICATION	1b RESTRICTIVE MARKINGS
2a SECURITY CLASSIFICATION AUTHORITY	3 DISTRIBUTION / AVAILABILITY OF REPORT
2b DECLASSIFICATION / DOWNGRADING SCHEDULE Unclassified	Approved for Public Release; Distribution Unlimited
4 PERFORMING ORGANIZATION REPORT NUMBER(S) BRL-TR- 3059	5 MONITORING ORGANIZATION REPORT NUMBER(S)
6a NAME OF PERFORMING ORGANIZATION US Army Ballistic Research Laboratory 6b OFFICE SYMBOL (If applicable) SLCBR-IB-A	7a NAME OF MONITORING ORGANIZATION
6c ADDRESS (City, State, and ZIP Code) Aberdeen Proving Ground, MD 21005-5066	7b ADDRESS (City, State, and ZIP Code)
8a NAME OF FUNDING / SPONSORING ORGANIZATION 8b OFFICE SYMBOL (If applicable)	9 PROCUREMENT INSTRUMENT IDENTIFICATION NUMBER
8c ADDRESS (City, State, and ZIP Code)	10 SOURCE OF FUNDING NUMBERS

PROGRAM ELEMENT NO.	PROJECT NO.	TASK NO.	WORK UNIT ACCESSION NO.
AH43	1L161102AH43	00	00

11 TITLE (Include Security Classification)
Calculated Gun Interior Ballistic Effects of In-Depth Burning of VHBR Propellant

12 PERSONAL AUTHOR(S)
Frederick W. Robbins and David L. Kruczynski

13a TYPE OF REPORT	13b TIME COVERED	14. DATE OF REPORT (Year, Month, Day)	15. PAGE COUNT
Technical Report	FROM Jun 88 TO Jun 89		

16. SUPPLEMENTARY NOTATION

17 COSATI CODES			18. SUBJECT TERMS (Continue on reverse if necessary and identify by block number)
FIELD	GROUP	SUB-GROUP	
19	06		VHBR Modeling, Monolithic Charge, In-Depth Burning

19 ABSTRACT (Continue on reverse if necessary and identify by block number)

Very High Burning Rate (VHBR) propellants exhibit sufficiently high burning rates to motivate consideration of a charge consisting of single-perforated monolithic grain. If the outside surfaces, including the ends, of such a grain were inhibited, the result would be a highly progressive grain whose performance could be quite attractive.

The VHBR picture is complicated, however, by the fact that some of these propellants seem to burn not only on the surface but also at some depth into the surface, so that they have an extended reaction zone. This paper details the development of a lumped parameter interior ballistic code which permits an examination of the ballistic effects of in-depth propellant combustion. It is concluded that if in-depth burning occurs in a reproducible manner, and if the grain is properly designed so that it is fully burned at the time of shot ejection, then the performance improvement over that expected from a conventional charge for the same gun is significant.

20. DISTRIBUTION / AVAILABILITY OF ABSTRACT	21 ABSTRACT SECURITY CLASSIFICATION
☒ UNCLASSIFIED/UNLIMITED ☐ SAME AS RPT ☐ DTIC USERS	Unclassified
22a. NAME OF RESPONSIBLE INDIVIDUAL Frederick W. Robbins	22b TELEPHONE (Include Area Code) (301) 278-6201
	22c. OFFICE SYMBOL SLCBR-IB-A

DD Form 1473, JUN 86 Previous editions are obsolete.

SECURITY CLASSIFICATION OF THIS PAGE
UNCLASSIFIED

INTENTIONALLY LEFT BLANK.

TABLE OF CONTENTS

INTENTIONALLY LEFT BLANK.

LIST OF FIGURES

Figure Page

INTENTIONALLY LEFT BLANK.

LIST OF TABLES

INTENTIONALLY LEFT BLANK.

I. INTRODUCTION

A large single-perforated monolithic grain comprised of Very High Burning Rate (VHBR)[1] propellant holds the promise of significant increases in performance in ballistic applications. It has been theorized by several researchers[1,2] that propellants with very high burning rates may be exhibiting a phenomenon in which burning takes place at some depth into the propellant simultaneously with surface burning. This phenomenon, referred to as "porous burning", if real, could have a significant impact on the performance of this family of propellants.

This study attempts to quantify these effects by modifying a current interior ballistic code to include a representation of this porous burning effect. The code not only allows a representation of porous burning but is generic enough to simulate any condition in which additional surface area beyond that traditionally expected becomes available during the burning process. This could happen as a result of porous burning, surface cracks, bubbles, or other irregularities in the propellant. For this report, the term "in-depth" burning is used to describe this generic surface-increasing effect.

II. THEORY

Most lumped parameter interior ballistic computer codes require the mass of propellant burned as a function of time. Then using an equation of state to get the mean pressure and an analytic formulation to get the projectile base pressure from the mean pressure, the code calculates the inbore projectile acceleration, velocity, and distance traveled. One approach (and the one we will follow) is to get the time rate of change of the mass of propellant burned from $\dot{m} = \rho S \frac{dx}{dt}$ and integrate this numerically to get the mass of propellant burned. Here $\dot{m}$ is the time rate of change of the mass of propellant burned, ρ is the density of the solid propellant (assumed constant), S is the total surface area of the burning propellant, and $\frac{dx}{dt}$ is the linear burning rate of the propellant.

The modeling problem for in-depth burning is to find a way to represent the surface area involved in the volume associated with the in-depth burning as well as that which would normally be associated with burning normal to the propellant surfaces. In this paper we will get the total surface area from normal surface areas as well as the surface associated with a volume by assuming it can be modeled by $S = S_o + S_a DM$. Here, S is the total surface area. S_o is the surface area associated with surface burning of the propellant. S_o is defined to be the surface that would be determined from the grain geometry, with burning normal to all burning surfaces, for the current mass of propellant burned. $S_a DM$ is the surface area associated with the in-depth burning volume, and we shall call this surface area S_v. D is the effective depth for which in-depth burning is hypothesized to occur and can be a function of any variable. In this paper, D is considered constant during any computation. S_a is the effective surface area such that the product of S_a and D is the volume in which in-depth burning is occurring. M is the surface area

per unit volume such that S_aDM, S_v, is the extra surface on which burning will occur within the in-depth burning volume. M may be thought of as the factor that describes the degree of porosity of the porous volume. M can also be a function of any variable, but for this paper, M will be kept constant.

All the subsequent calculations will be done for a single-perforated monolithic grain with the ends and lateral surfaces inhibited. The grain fills most of the gun chamber. For this geometry S_a can be defined in terms of the current perforation surface S_o. It can be shown that $S_a = S_o \frac{(D + 2R)}{(2R)}$, where S_a is the multiplier of the in-depth burning distance, D, such that S_aD gives the volume undergoing in-depth burning, and R is the instantaneous radius of the perforation.

Figure 1 gives a graphic representation of some of the parameters discussed above.

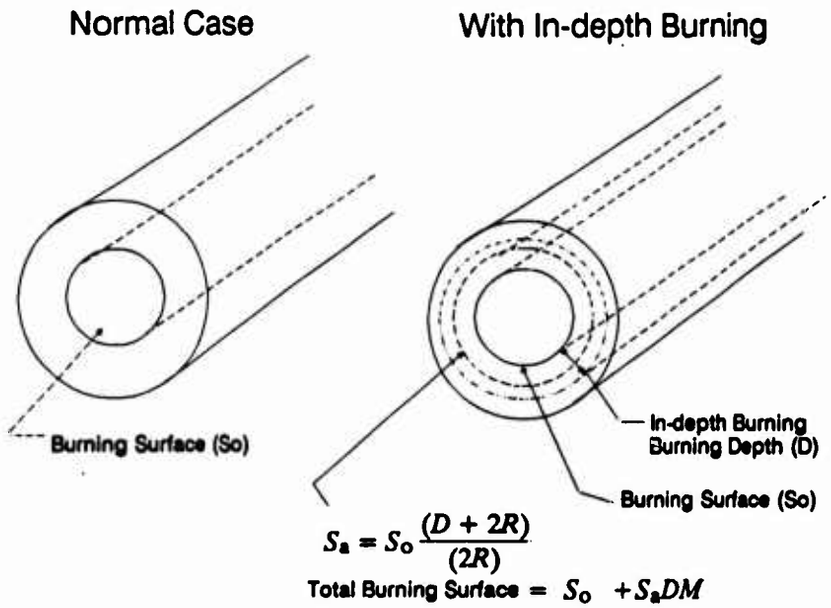

Figure 1. In-depth Burning Parameters

III. COMPUTATIONS

The lumped parameter interior ballistic code used for the following calculations is a version of IBRGA[3] (which uses The Technical Cooperative Program (TTCP) model) modified for the above in-depth analysis (a listing, input, output, and a short description of the input are given in Appendices A, B, C, and D, respectively). The calculations are performed for a single-perforated monolithic grain which burns a) only on the perforation surface or b) on the perforation surface and in an in-depth volume which extends from the perforation surface. The purpose of the calculations will be to assess the geometric effects of in-depth burning on the progressive nature of an outside- and end-inhibited single-perforated monolithic grain. It is assumed that the burning rate of the propellant can be

controlled in manufacture such that for given grain and gun dimensions any desired maximum breech pressure can be achieved. That is, for any grain dimensions and in-depth burning, the burning rate will be varied to achieve the desired maximum breech pressure. The effects of in-depth burning will be assessed by comparing muzzle velocities for the same grain configuration with the same maximum breech pressure but with different effective in-depth burning depths *(D)* and surface areas per unit volume *(M)*.

Data for the propellant used in all the calculations are given in Table 1. Information on the gun systems is given in Tables 2 and 3. The two gun systems were chosen to look at typical low and high ratios of propellant-charge-weight to projectile-weight.

The mass of the propellant grain was calculated to give one grain for each perforation diameter. The outside grain diameter was 15 cm for both gun systems. The calculations used the Lagrange gradient with nominal heat loss, no recoil, no resistive forces, a burning rate exponent of one, and all burning propellant surfaces burning at time zero at ambient pressure.

Table 1. Propellant Characteristics

Impetus of propellant	**1160 J/g**
Flame temperature	**3141 K**
Covolume	**1.12 cm cu/g**
Density	**1.53 g/cm cu**
Gamma	**1.23**

Table 2. Small Gun System
(chamber vol 9832.24 cm cu)

Bore diameter	**12.7 cm**
Travel	**457.2 cm**
Projectile mass	**9.796 kg**
Propellant grain length	**50.0 cm**
Maxium breech pressure	**517.0 MPa**

Table 3. Large Gun System
(chamber vol 22,941 cm cu)

Bore diameter	**15.64 cm**
Travel	**698.5 cm**
Projectile mass	**43.54 kg**
Propellant grain length	**109.22 cm**
Maxium breech pressure	**345.0 MPa**

The effects of in-depth burning as modeled here will be caused by the decrease in surface area in the in-depth burning volume (S_V) as the in-depth burning volume intersects the outer grain surface and starts to get smaller. Figure 2 illustrates this effect where (a) shows the in-depth burning volume before intersection with the outer surface, (b) shows the increased in-depth burning volume just at its intersection with the outer surface and (c) shows the decrease in the in-depth volume some time after its intersection with the outer surface.

This is further illustrated in Figure 3 where the surface area of the perforation (S_o) and the surface associated with the in-depth burning volume (S_v) versus distance burned into the grain is given for different effective in-depth burning depths. The curves were generated for no in-depth burning depth ($D=0$), the in-depth burning depth set to half of the web ($D=3.25$ cm) and for the in-depth burning depth set to the web ($D=6.5$ cm).

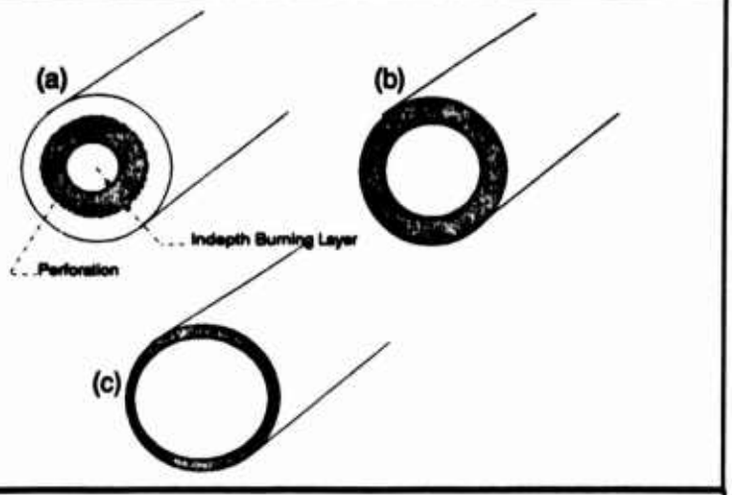

Figure 2. Surface Area Changes During In-Depth Burning

Table 4 demonstrates the wide range of surface areas we get from different values of the surface area per unit volume *(M)* for different in-depth burning depths *(D)*. To provide a physical comparison, the surface area in the in-depth burning volume (S_v) is referenced to the perforation surface area (S_o). These calculations were done for an

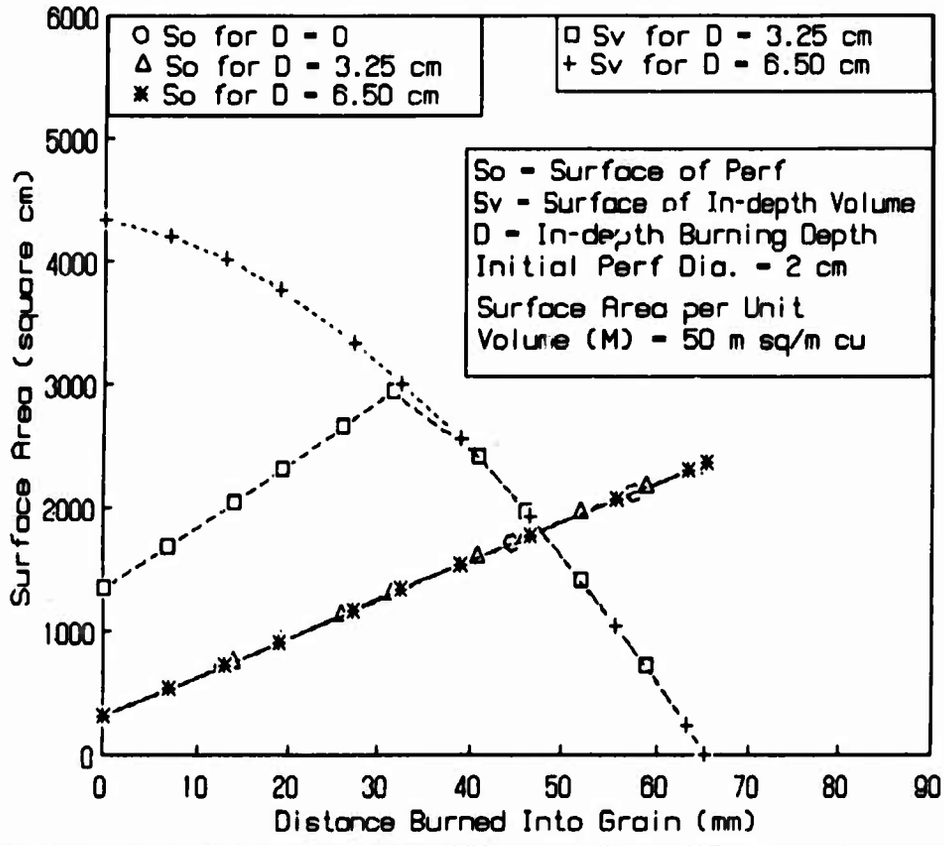

Figure 3. Surface Area Changes During In-depth Burning

average perforation diameter of 9 cm, but the ratios do not change much for larger or smaller perforations.

If in-depth burning occurs, and if the increase in surface area in that in-depth burning volume is small, then the model predicts a degradation in velocity of only a few percent. For example, a 2-cm-diameter perforation in the small gun system with no in-depth burning gives a velocity of 1713 m/s. With $M = 1\ m^2/m^3$, so that $\frac{S_v}{S_o}$ is very small, and with the burning depth *(D)* equal to the web, 6.5 cm, we get a velocity of 1648 m/s, a decrease of only 3.8 percent.

Table 4. Ratio of In-depth Surface to Perforation Surface (Sv/So)

in-depth Burning depth(D) (m)	Surface Volume Multiplier (M) Surface Area Per Unit Volume (m sq/m cu) 1	5	50	500
0.001	0.001	0.005	0.050	0.50
0.005	0.005	0.026	0.264	2.64
0.010	0.011	0.055	0.555	5.55
0.015	0.018	0.088	0.875	8.75
0.030	0.040	0.200	2.00	20.0

For $M = 50\ m^2/m^3$, so that $\frac{S_v}{S_o}$ is about unity, the initial perforation diameter for which complete combustion of the propellant grain will occur becomes larger than 2 cm. As the depth of penetration of the in-depth burning increases there is an increase in the initial diameter of the perforation for which complete burnout of the propellant will occur. If the effective in-depth burning depth of the in-depth burning volume is made equal to the web of the propellant grain (the largest it can be), then the initial perforation diameter for which burnout will occur is 10.0 cm for the large gun system and 9.36 cm for the small gun system.

For $M = 500\ m^2/m^3$, so that $\frac{S_v}{S_o}$ is larger than one, the perforation diameter for which burnout will occur when the depth of penetration of the in-depth burning is made equal to the web of the propellant grain is 11.7 cm for the large gun system and 11.3 for the small gun system.

A plot of the velocity versus the perforation diameter with no in-depth burning is shown for both the small and large gun systems in Figure 4. The optimal velocity for the systems is seen to be when the perforation diameter is small,

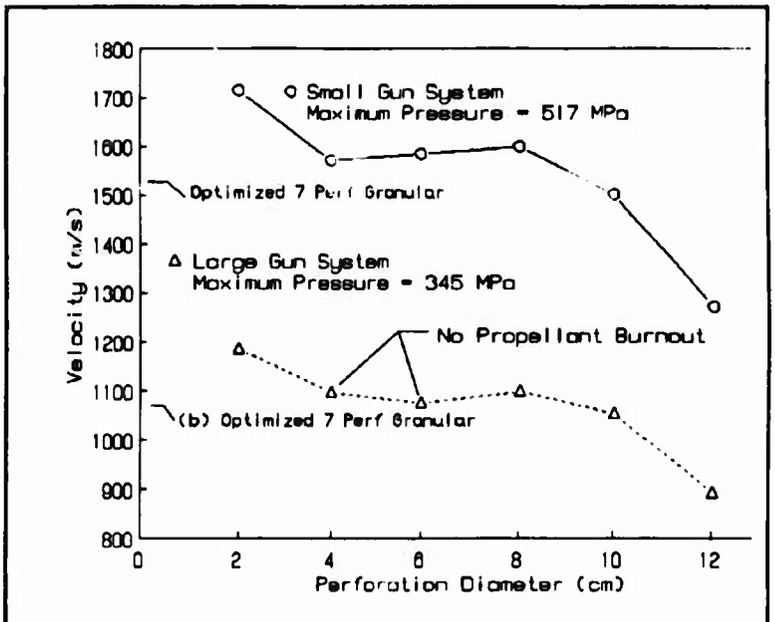

Figure 4. Velocity vs. Perf Diameter (No In-depth Burn)

about 1-2 cm. The smaller local maxima in velocity, seen for larger perforation diameters, occurs because of the constraint of having only one grain. With only one grain with a constant outer diameter, for a large perforation, the grain acts like a single-perforated monolithic stick configuration. With a large perforation diameter the progressivity is small, with the optimal velocity occurring for grains which burn out before muzzle exit. For small perforations, the surface area near maximum breech pressure increases nearly as fast as the volume is increasing, resulting in the pressure being near maximum breech pressure before and up to burnout.

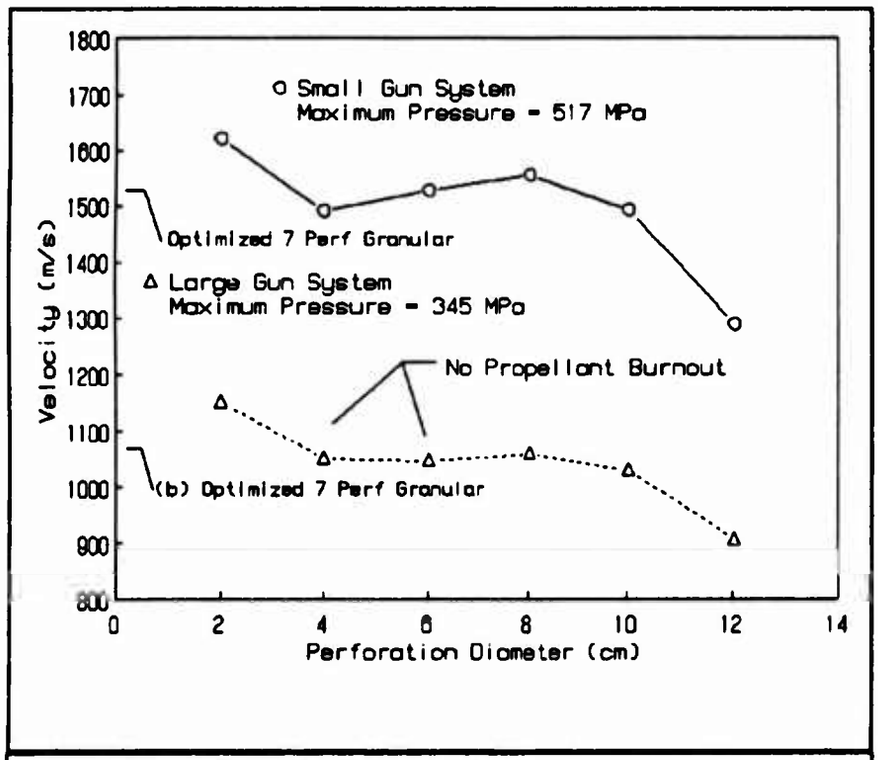

Figure 5. Velocity vs. Perf Diameter (D = 15 mm)

Figure 5 is the same plot as Figure 4 of velocity versus perforation diameter with the in-depth burning depth *(D)* being 1.5 cm and the surface area per unit volume *(M)* being 50 m^2/m^3. The general shape and magnitude of the curves are about the same.

Table 5. Velocities and Burnout Conditions - Small Gun

Surface Volume Multiplier - M

In-depth Burning Depth (D) (mm)	1		5		50		500	
	Velocity (m/s)	Fraction Burned	Velocity (m/s)	Fraction Burned	Velocity (m/s)	Fraction Burned	Velocity (m/s)	Fraction Burned
0	1713	1	1713	1	1713	1	1713	1
1	1713	1	1713	1	1713	1	1712	1
5	1713	1	1712	1	1709	1	1682	1
10	1712	1	1711	1	1683	1	1589	0.93
15	1712	1	1707	1	1619	0.99	1497	0.81
30	1705	1	1653	1	1389	0.64	1304	0.54
45	1685	1	1479	0.81	1190	0.42	1137	0.37
65	1648	1	1282	0.55	999	0.27	947	0.24

Fraction Burned = fraction propellant burned at projectile exit
Cases where fraction is less than one are highlighted
Optimized velocity for a seven perforation granular charge using IBRGA = 1531 m/s

Table 6. Velocities and Burnout Conditions - Large Gun

Surface Volume Multiplier - M

In-depth Burning Depth (D) (mm)	1		5		50		500	
	Velocity (m/s)	Fraction Burned	Velocity (m/s)	Fraction Burned	Velocity (m/s)	Fraction Burned	Velocity (m/s)	Fraction Burned
0	1185	1	1185	1	1185	1	1185	1
1	1185	1	1185	1	1185	1	1186	1
5	1185	1	1186	1	1186	1	1181	1
10	1186	1	1187	1	1181	1	1136	0.93
15	1186	1	1186	1	1149	0.97	1086	0.82
30	1186	1	1161	1	1017	0.86	966	0.56
45	1180	1	1086	0.81	881	0.44	846	0.35
65	1163	1	957	0.59	752	0.29	721	0.26

Fraction Burned = fraction propellant burned at projectile exit
Cases where fraction is less than one are highlighted
Optimized velocity for a seven perforation granular charge using IBRGA = 1074 m/s

The effects of in-depth burning on near-optimal grain configurations (2-cm initial perforation diameter) for the same maximum pressure are given in Tables 5 and 6. The calculations were performed by varying the burning rate to get a specified maximum breech pressure. It is seen that for small values of surface area per unit volume *(M)* that the velocity drops only a few percent with even large changes in the in-depth burning depth. For larger values of surface area per unit volume *(M)* the velocity still does not drop very much until all of the propellant does not burn up completely, as evidenced by the mass fraction burned at projectile exit being less than one.

Table 7. Effects on Maximum Breech Pressure - Small Gun System

Indepth Burning Depth (m)	Pressure (Mpa) Surface Volume Multiplier 1	5	50
0.0	517	517	517
0.001	522	545	1039
0.005	549	742	
0.015	664	2359	

The effects of in-depth burning occurring for a designed grain with no expected in-depth burning (the burning rate of the propellant remains the same) are given in Table 7. There is a large effect on the maximum pressure for small increases in surface area in the in-depth burning volume.

The missing data in Table 7 are from cases when the pressure exceeded the limits of the equation of state.

IV. DISCUSSION

The incorporation of an in-depth burning model into the lumped parameter interior ballistic computer code was done such that the effective in-depth burning depth *(D)* could be varied as well as the surface area per unit volume *(M)*. A time and a threshold pressure condition was also imposed, both of which must be exceeded, before in-depth burning commences. Also the burning rate for the in-depth burning volume may be different from the burning rate before in-depth burning starts. In all simulations reported, in-depth burning started at time zero and atmospheric pressure. During any single simulation, a constant effective in-depth burning depth and a constant surface area per unit volume were used. The burning rate for the surface in the in-depth burning volume (S_V) was the same as that before in-depth burning started. It is believed that this model, with the proper in-depth burning characteristics, will simulate, at least in direction and relative magnitude, most situations in which in-depth burning may occur (e.g., porous burning, rough burning surfaces, crack formation, and grain breakup).

The purpose of the calculations is to assess the geometric consequences of in-depth burning for a single-perforated outside- and end-inhibited monolithic grain. The calculations indicate that there are two major effects, assuming that the burning rate of the propellant can be adjusted to achieve a desired maximum breech pressure. These effects

are due to the decrease of the in-depth burning volume after its intersection with the outside of the grain and effects due to the grain's not burning out. If the burning rate is kept the same and in-depth burning occurs, then for a small increase in surface in the in-depth volume (S_V), there is a large increase in maximum breech pressure.

The interest in a large single-perforated monolithic grain which burns only on the perforation is evident when we compare the increase in velocity over that of an optimized 7-perforated granular charge. For the small gun system the velocity increase is from 1531 m/s to 1713 m/s, an increase of 11.9 percent, and for the large gun system the velocity increases from 1074 m/s to 1185 m/s, an increase of 10.3%. This large increase in velocity requires that the burning rate of the monolithic grain be two orders of magnitude larger (because of the small surface area of the grain) than the burning rate for normal propellant. This large burning rate induces a large sensitivity to small increases in burning surface area as can be seen in Table 5. This results in large increase in maximum breech pressure for small increases in the in-depth burning surface.

The effects of the in-depth volume's intersecting the outer surface of the grain and then the in-depth volume's decreasing along with its surface area (as long as burnout still occurs) result in a velocity decrease on the order of 4 percent. Even with this decrease, there would still be an increase in velocity over a standard 7-perforated granular charge.

A major drop in velocity is seen to occur (Tables 5 & 6) when the charge does not burn out completely. Burnout of the propellant does not occur because the burning rate must be lowered (to stay below a given maximum breech pressure) as surface area is increased in the in-depth burning volume. With this decreased burning rate, and for large in-depth burning depths, the surface area decreases after intersection with the outer diameter, leading to lower mass generation. This effect is similar to the slivering event in multiperforated granular propellant.

All of these effects from in-depth burning would suggest that the use of one large single-perforated outside- and end-inhibited monolithic grain would be viable even if in-depth burning occurs, if the burning rate can be controlled and the amount (if any) of in-depth burning is reproducible and definable.

V. CONCLUSIONS

There are three major consequences if in-depth burning is occurring in a large mono-perforated outside- and end-inhibited grain

- *If the grain is properly designed, then little degradation in performance accompanies in-depth burning.*

- *For efficient grain design, the amount of in-depth burning must be small enough that grain burnout occurs.*

- *If the grain is designed for a given burning rate and more in-depth burning occurs than is designed for, then much larger than expected maximum breech pressures are probable.*

A simple versatile model for in-depth burning has been incorporated into a standard lumped parameter interior ballistic code.

INTENTIONALLY LEFT BLANK.

ACKNOWLEDGMENTS

The authors wish to thank Mr. A.W. Horst, Dr. K. White, Dr. A. A. Juhasz, Dr. T. C. Minor, and Mr. R. Deas for helpful discussions and technical insight. We also wish to thank Mr. T. Raab and Ms. K. Cieslewicz for performing many computer runs and code modifications. Ms. K. E. Meyers is acknowledged for the preparation and editing of the technical drawings and manuscript.

REFERENCES

1. White K. J., McCoy D. G., Doali J. O., Aungst W. P., Bowman R. E. and Juhasz A. A.,"Closed Chamber Burning Characteristics of New VHBR Formulations", BRL-MR-3471, USA Ballistic Research Laboratory, Aberdeen Proving Ground, MD., October 1985.

2. Fifer R. A. and Cole J. E., "Transitions From Laminar Burning for Porous Crystalline Explosives", 17th International Symposium on Detonation, pp 164-174, June 1981.

3. Robbins F. W. and Raab T. S., "A Lumped-Parameter Interior Ballistic Computer Code Using The TTCP Model", BRL-MR-3710, USA Ballistic Research Laboratory, Aberdeen Proving Ground, MD, November 1988.

INTENTIONALLY LEFT BLANK.

APPENDIX A
Listing of Program

INTENTIONALLY LEFT BLANK.

```
      program ibrgam1
      character bdfile*10,outfil*10
      dimension br(10),trav(10),rp(10),tr(10),forcp(10),tempp(10),covp(
     &10),grainn(10)
      dimension chwp(10),rhop(10),gamap(10),nperfs(10),glenp(10),pdpi(10
     &),p dpo(10),gdiap(10),dbpcp(10),alpha(10,10),beta(10,10),
     &pres(10,10),tbo(10)
      dimension a(4),b(4),ak(4),d(20),y(20),p(20),z(20),frac(10),surf(10
     &),nbr(10),ibo(10),ipdb(10)
      dimension nbrn(10)
     &,betan(10,10),alphan(10,10),presn(10,10),idbs(10),td(10),pdb(10),
     &dpen(10),smult(10)
      real lambda,j1zp,j2zp,j3zp,j4zp
      dimension chdist(5),chdiam(5),bint(4)
      data idbs/0,0,0,0,0,0,0,0,0,0/
c     call gettim(ihr,imin,isec,ihuns)
      pi=3.141592654
      write(*,15)
15    format(' input name of data file to be used as input ')
      read(*,10)bdfile
10    format(a10)
      open(unit=2,err=999,file=bdfile,status='old',iostat=ios)
      write(*,25)
25    format(' input name of output file ')
      read(*,10)outfil
      open(unit=3,err=998,file=outfil,status='new')
      write(3,2)bdfile
2     format(1x,' USING INPUT FILE ',a10)
      read(2,*,end=20,err=30)cham,grve,aland,glr,twst,travp,igrad
      if(igrad.gt.1)go to 51
      write(3,55)
55    format(1x,'using Lagrange pressure gradient')
      go to 52
c     define chambrage assumes nchpts=number of points to define
c     chamber > or = 2 < or = 5 (?),chdiam(I) defines chamber diameter
c     at chdist (I) chamber distance.  chdiam(nchpts) is assumed to be
c     the bore diameter and chdist(i) is assumed to be 0, i.e. at the
c     breech. Assumes truncated cones.
51    write(3,47,err=30)
47    format(1x,'Using chambrage pressure gradient')
      read(2,*,end=20,err=30)nchpts,(chdist(I),chdiam(I),I=1,nchpts)
      write(3,53,err=30)(chdist(I),chdiam(I),I=1,nchpts)
53    format(///,'   chamber distance cm   chamber diameter cm',/(5x,e14
     &.6,5x,e14.6))
      do 54 I=1,nchpts
      chdist(I)=0.01*chdist(I)
54    chdiam(I)=0.01*chdiam(I)
c     calculate chamber integrals and volume
      if(nchpts.gt.5) write(3,44,err=30)
44    format(1x,'use first 5 points')
      if(nchpts.gt.5)nchpts=5
      bore=chdiam(nchpts)
      if(chdist(1).ne.0.0)write(3,45,err=30)
45    format(1x,' # points ? ')
      chdist(1)=0.0
      pi3=pi/3.0
      b1=0.0
      b2=0.0
      b3=0.0
```

```
      b4=0.0
      points=25.0
56    points=points+points
      step=chdist(nchpts)/points
      zz=0.0
      bint(1)=0.0
      bint(3)=0.0
      bint(4)=0.0
      bvol=0.0
      r2=0.5*chdiam(1)
      k=1
      j=int(points+0.5)
      do 57 I=1,j
      zz=zz+step
      if(k.eq.nchpts-1)go to 46
      do 58 I1=k,nchpts-1
      if(zz.gt.chdist(I1).and. zz.lt.chdist(I1+1))go to 59
58    continue
      I1=nchpts-1
59    k=I1
46    diam=(zz-chdist(k))/(chdist(k+1)-chdist(k))
      diam=chdiam(k)+diam*(chdiam(k+1)-chdiam(k))
      r1=0.5*diam
      area=pi*(r1+r2)*(r1+r2)/4.
      bvol=bvol+step*pi3*(r1*r1+r1*r2+r2*r2)
      bint(1)=bint(1)+step*bvol/area
      bint(3)=bint(3)+step*area*bint(1)
      bint(4)=bint(4)+step*bvol*bvol/area
57    r2=r1
      temp=abs(1.0-b1/bint(1))
      if(abs(1.0-b3/bint(3)).gt.temp)temp=abs(1.0-b3/bint(3))
      if(abs(1.0-b4/bint(4)).gt.temp)temp=abs(1.0-b4/bint(4))
      if(temp.le.0.001)go to 41
      b1=bint(1)
      b3=bint(3)
      b4=bint(4)
      go to 56
41    cham=bvol*1.e6
c     write(3,47,err=30)bint(1),bint(3),bint(4)
c     format(1x,'bint 1 = ',e14.6,'  bint 3 = ',e14.6,'  bint 4 = ',e14.
c    &6)
      chmlen=chdist(nchpts)
52    write(3,40,err=30)cham,grve,aland,glr,twst,travp
40    format(1x,'chamber volume cm**3',e14.6,/'  groove diam cm',e14.6,/
     &' land diam cm',e14.6,/'  groove/land ratio',e14.6,/'  twist turns
     &/caliber ',e14.6,/'  projectile travel cm',e14.6///)
      cham=cham*1.e-6
      grve=grve*1.e-2
      aland=aland*1.e-2
      travp=travp*1.e-2
      read(2,*,end=20,err=30)prwt,iair,htfr,pgas
      write(3,50,err=30)prwt,iair,htfr,pgas
50    format(1x,'projectile mass kg',e14.6,/'  switch to calculate energ
     &y lost to air resistance J',i2,/'  fraction of work against bore u
     &sed to heat the tube',e14.6/1x,' gas pressure Pa' ,e14.6)

      read(2,*,end=20,err=30)npts,(br(i),trav(i),i=1,npts)
      write(3,60,err=30)npts,(br(i),trav(i),i=1,npts)
60    format(1x,'number barrel resistance points',i2,/'  bore resistance
     & MPa - travel cm'/(1x,e14.6,e14.6))
```

```
      write(3,65)
      do 62 i=1,npts
      br(i)=br(i)*1.e6
      trav(i)=trav(i)*1.e-2
62    continue
65    format(1x)
      read(2,*,end=20,err=30)rcwt,nrp,(rp(i),tr(i),i=1,nrp)
      write(3,70,err=30)rcwt,nrp,(rp(i),tr(i),i=1,nrp)
70    format(1x,'  mass of recoiling parts kg',e14.6,/'  number of recoi
     &l point pairs',i2,/'  recoil force N','  recoil time sec'/,(1x,e14
     &.6,3x,e14.6))
      write(3,65)
      read(2,*,end=20,err=30)ho,tshl,cshl,twal,hl,rhocs
      write(3,75,err=30)ho,tshl,cshl,twal,hl,rhocs
75    format(1x,'  free convective heat transfer coefficient w/cm**2 k',
     &e14.6,/'  chamber wall thickness cm',e14.6,/'  heat capacity of st
     &eel of chamber wall j/g k',e14.6,/'  initial temperature of chambe
     &r wall k',e14.6,/'  heat loss coefficient',e14.6,/'  density of ch
     &amber wall steel g/cm**3',e14.6//)
      ho=ho/1.e-4
      tshl=tshl*1.e-2
      cshl=cshl*1.e+3
      rhocs=rhocs*1.e-3/1.e-6
      read(2,*,end=20,err=30)forcig,covi,tempi,chwi,gamai
      write(3,85,err=30)forcig,covi,tempi,chwi,gamai
85    format(1x,'  impetus of igniter propellant J/g',e14.6,/'  covolume
     & of igniter cm**3/g',e14.6,/'  adiabatic flame temperature of igni
     &ter propellant k',e14.6,/'  initial mass of igniter kg',e14.6,/' r
     &atio of specific heats for igniter',e14.6//)
      forcig=forcig*1.e+3
      covi=covi*1.e-6/1.e-3
      read(2,*,end=20,err=30)nprop
      tmpi=0.0
      do 99 i=1,nprop
      read(2,*,end=20,err=30)idbs(i),forcp(i),tempp(i),covp(i),chwp(i),
     &rhop(i),gamap(i),nperfs(i),glenp(i),pdpi(i),pdpo(i),gdiap(i),dbpcp
     &(i),ingc
      write(3,95,err=30)i,forcp(i),tempp(i),covp(i),chwp(i)
     &,rhop(i),gamap(i),nperfs(i),glenp(i),pdpi(i),pdpo(i),gdiap(i),dbpc
     &p(i)
95    format((' for propellant number ',i2,/'  impetus of propellant J/g
     &',e14.6,/'  adiabatic temperature of propellant K',e14.6,/'  covol
     &ume of propellant cm**3/g',e14.6/'  initial mass of propellant kg'
     &,e14.6/'  density of propellant g/cm**3',e14.6/'  ratio of specifi
     &c heats for propellant',e14.6/'  number of perforations of propell
     &ant',i2/'  length of propellant grain cm',e14.6/'  diameter of inn
     &er perforation in propellant grains cm',e14.6/'  diameter of outer
     &perforation of propellant grains cm',e14.6/'  outside diameter of
     &propellant grain cm',e14.6/'  distance between perf centers cm',e1
     &4.6)//)
      if(INGC.ne.1)go to 191
      if(nperfs(I).ne.-1)go to 191
      chwp(I)=pi*(gdiap(I)**2-pdpo(I)**2)/4.0*glenp(i)*rhop(I)/1000.
      write(3,192)chwp(I)
192   format(1x,'propellant wt changed to ',e14.6,' kg')
191   if(idbs(i).eq.0)go to 96
      read(2,*,end=20,err=30)td(i),pdb(i),dpen(i),smult(i)
      write(3,98,err=30)td(i),pdb(i),dpen(i),smult(i)
98    format(' IN DEPTH BURNING WILL OCCUR WHEN TIME IS GREATER THAN ',e
     &14.6,' MSEC'/'  AND PRESSURE IS GREATER THAN ',E14.6,'MPa'/' INITI
```

```
     &AL DEPTH BURNT PENETRATION mm ',e14.6,/' AND INITIAL SURFACE AREA/
     &UNIT VOLUME m**2/m**3 ',e14.6,/)
96    forcp(i)=forcp(i)*1.e+3
      covp(i)=covp(i)*1.e-6/1.e-3
      rhop(i)=rhop(i)*1.e-3/1.e-6
      td(i)=td(i)*0.001
      pdb(i)=pdb(i)*1.e6
      dpen(i)=dpen(i)*0.001
      glenp(i)=glenp(i)*0.01
      pdpi(i)=pdpi(i)*0.01
      pdpo(i)=pdpo(i)*0.01
      gdiap(i)=gdiap(i)*0.01
      dbpcp(i)=dbpcp(i)*0.01
      tmpi=tmpi+chwp(i)
      if(nperfs(i).eq.-1)go to 91
      if(nperfs(i).eq.-11) go to 92
      call prf017(pdpo(i),pdpi(i),gdiap(i),dbpcp(i),glenp(i),
     & surf(i),frac(i),0.0,nperfs(i),u)
      go to 93
91    call mono(pdpo(i),gdiap(i),glenp(i),surf(i),frac(i),0.0,u)
      go to 93
92    call cig(gdiap(i),glenp(i),surf(i),frac(i),0.0,u)
93    grainn(i)=chwp(i)/(rhop(i)*u)
      write(3,94,err=30)i,grainn(i)
94    format(' the calculated number of grains for propellant ',i2,
     & ' is ',e14.6)
99    continue
      tmpi=tmpi+chwi
      do 97 j=1,nprop
      read(2,*,end=20,err=30)nbr(j),(alpha(j,i),beta(j,i),pres(j,i),
     &i=1,nbr(j))
      write(3,110,err=30)j,nbr(j),(alpha(j,i),beta(j,i),pres(j,i),
     &i=1,nbr(j))
110   format(1x,' for propellant ',i2,' the number of burning rate point
     &s is',i2/3x,'  exponent',8x,' coefficient',10x,'  pressure'/5x,'-'
     &,15x,'cm/sec-mpa**ai',10x,'mpa',/(1x,e14.6,5x,e14.6,15x,e14.6))
      if(idbs(j).eq.0)go to 111
      read(2,*,end=20,err=30)nbrn(j),(alphan(j,i),betan(j,i),presn(j,i),
     &i=1,nbrn(j))
      write(3,116,err=30)nbrn(j),(alphan(j,i),betan(j,i),presn(j,i),i=1,
     & nbrn(j))
116   format(' THE INTERIOR BURNING SURFACE FOR IN-DEPTH BURNING WILL RE
     &GRESS ACCORDING TO '/' number of burning rate points',i2/3x,' expo
     &nent',8x,' coefficient',10x,'  pressure'/5x,'-',15x,'cm/sec-mpa**a
     &i',10x,'mpa',/(1x,e14.6,5x,e14.6,15x,e14.6))
111   do 112 i=1,nbr(j)
      beta(j,i)=beta(j,i)*1.e-2
      betan(j,i)=betan(j,i)*1.e-2
      pres(j,i)=pres(j,i)*1.e6
      presn(j,i)=presn(j,i)*1.e6
112   continue
97    continue
      write(3,65)
      read(2,*,end=20,err=30)deltat,deltap,tstop
      write(3,120,err=30)deltat,deltap,tstop
120   format(1x,'time increment msec',e14.6,'  print increment msec',e14
     &.6/1x,'time to stop calculation msec ',e14.6)
      write(*,130)
      deltat=deltat*0.001
      deltap=deltap*0.001
```

```
      tstop=tstop*.001
130   format(1x,'normal end')
      if(igrad.gt.1)go to 131
      bore=(glr*grve*grve+aland*aland)/(glr+1.)
      bore=sqrt(bore)
131   areab=pi*bore*bore/4.
      lambda=1./((13.2+4.*log10(100.*bore))**2)
      pmaxm=0.0
      pmaxbr=0.0
      pmaxba=0.0
      tpmaxm=0.0
      tpmaxbr=0.0
      tpmaxba=0.0
      tpmax=0.0
      a(1)=0.5
      a(2)=1.-sqrt(2.)/2.
      a(3)=1.+sqrt(2.)/2.
      a(4)=1./6.
      b(1)=2.
      b(2)=1.
      b(3)=1.
      b(4)=2.
      ak(1)=0.5
      ak(2)=a(2)
      ak(3)=a(3)
      ak(4)=0.5
      vp0=0.0
      tr0=0.0
      tcw=0.0
      ipdbm=0
      ipdbc=0
      do 5 i=1,nprop
      ipdb(i)=0
      ibo(i)=0
      tbo(i)=0
  5   vp0=chwp(i)/rhop(i)+vp0
      volgi=cham-vp0-chwi*covi
      pmean=forcig*chwi/volgi
      volg=volgi
      volgi=volgi+vp0
      wallt=twal
      ptime=0.0
      ibrp=8
      IMF=IBRP+NPROP
      z(3)=1.
      y(3)=0.
      ngrain=0.
      nde=ibrp+nprop+NPROP
      write(3,132)areab,pmean,vp0,volgi
132   format(1x,'area bore m^2 ',e16.6,' pressure from ign pa',e16.6,/
     &1x,' volume of unburnt prop m^3 ',e16.6,' init cham vol-cov ign m
     &^3 ',e16.6)
      write(3,6)
6     format(1x,'   time       acc        vel        dis        mpress
     &   pbase      pbrch    ')
      iswl=0
19    continue
      do 11 J=1,4
c     FIND BARREL RESISTANCE
      do 201 k=2,npts
```

```
      if(y(2)+y(7).ge.trav(k))go to 201
      go to 203
201   continue
      k=npts
203   resp=(trav(k)-y(2)-y(7))/(trav(k)-trav(k-1))
      resp=br(k)-resp*(br(k)-br(k-1))
c     FIND MASS FRACTION BURNING RATE
      do 211 k=1,nprop
      if(ibo(k).eq.1)goto211
      if(nperfs(k).eq.-1)go to 71
      if(nperfs(k).eq.-11)go to 72
      go to 73
71    continue
      if(idbs(k).eq.0)go to 74
      if(td(k).gt.t) go to 74
      if(ipdb(k).eq.1) go to 76
      if(pdb(k).gt.pmean)go to 74
      ipdb(k)=1
76    pddb=sqrt(gdiap(k)**2-4.*(chwp(k)-y(imf+k))/rhop(k)/grainn(k)/pi/
     &glenp(k))
      distsb=(pddb-pdpo(k))/2.
      call mono(pdpo(k),gdiap(k),glenp(k),surf(k),frac(k),distsb,u)
      if(dpen(k).gt.(gdiap(k)-pddb)/2.)dpen(k)=(gdiap(k)-pddb)/2.
      sa=(1.0+dpen(k)/pddb)
      surfsb=surf(k)*(sa)*dpen(k)*smult(k)+
     & surf(k)
      z(imf+k)=grainn(k)*rhop(k)*surfsb*z(ibrp+k)
c     write(3,204)pddb,distsb,dpen(k),surfsb,surf(k),sa
c204  format(1x,' perf diameter during in-depth burning',e14.6 /' distan
c    &ce burnt into grain perf ',e14.6/' depth of penetration',e14.6,' t
c    &otal surface',e14.6/' surface of perf',e14.6,' surface multiplier'
c    &,e14.6)
      if(surf(k).gt.1.e-10) go to 211
      ibo(k)=1
      tbo(k)=y(3)
      go to 211
74    call mono(pdpo(k),gdiap(k),glenp(k),surf(k),frac(k),y(ibrp+k),u)
      z(imf+k)=grainn(k)*rhop(k)*surf(k)*z(ibrp+k)
c     write(3,204)pddb,distsb,dpen(k),surfsb,surf(k),sa
      if(surf(k).gt.1.e-10) go to 211
      ibo(k)=1
      tbo(k)=y(3)
      go to 211
72    continue
      if(idbs(k).eq.0)go to 77
      if(td(k).lt.y(3)) go to 77
      if(ipdb(k).eq.1) go to 78
      if(pdb(k).lt.pmean)go to 77
      ipdb(k)=1
78    dblnth=(chwp(k)-y(imf+k))*4./gdiap(k)/gdiap(k)/pi/rhop(k)
       distsb= glenp(k)-dblnth
      call cig(gdiap(k),glenp(k),surf(k),frac(k),distsb,u)
      if(dpen(k).gt. bdlnth)dpen(k)=bdlnth
      surfsb=surf(k)*dpen(k)*smult(k)+
     & surf(k)
      z(imf+k)=grainn(k)*rhop(k)*surfsb*z(ibrp+k)
      if(surf(k).gt.1.e-10) go to 211
      ibo(k)=1
      tbo(k)=y(3)
      go to 211
```

```
77    call cig(gdiap(k),glenp(k),surf(k),frac(k),y(ibrp+k),u)
      z(imf+k)=grainn(k)*rhop(k)*surf(k)*z(ibrp+k)
      if(surf(k).lt.1.e-10) ibo(k)=1
      go to 211
73    call prf017(pdpo(k),pdpi(k),gdiap(k),dbpcp(k),glenp(k),surf(k),fra
     &c(k),y(ibrp+k),nperfs(k),u)
      Z(IMF+K)=GRAINN(K)*RHOP(K)*SURF(K)*Z(IBRP+K)
      if(surf(k).gt.1.e-10) go to 211
      ibo(k)=1
      tbo(k)=y(3)
211   continue
c     ENERGY LOSS TO PROJECTILE TRANSLATION
      elpt=prwt*y(1)*y(1)/2.
c     ENERGY LOSS DUE TO PROJECTILE ROTATION
      elpr=pi*pi*prwt*y(1)*y(1)/4.*twst*twst
c     ENERGY LOSS DUE TO GAS AND PROPELLANT MOTION
      if(igrad.le.1)go to 214
      pt=y(2)+y(7)
      vzp=bvol+areab*pt
      j4zp=bint(4)+((bvol+areab*pt)**3-bvol**3)/3./areab/areab
      elgpm=tmpi*y(1)*y(1)*areab*areab*j4zp/2./vzp/vzp/vzp
      go to 216
214   elgpm=tmpi*y(1)*y(1)/6.
c     ENERGY LOSS FROM BORE RESISTANCE
216   elbr=y(4)
      z(4)=areab*resp*y(1)
c     ENERGY LOSS DUE TO RECOIL
      elrc=rcwt*y(6)*y(6)/2.
c     ENERGY LOSS DUE TO HEAT LOSS
      areaw=cham/areab*pi*bore+2.*areab+pi*bore*(y(2)+y(7))
      avden=0.0
      avc=0.0
      avcp=0.0
      z18=0
      z19=0
      do 213 k=1,nprop
      z18=forcp(k)*gamap(k)*Y(IMF+K)/(gamap(k)-1.)/tempp(k)+z18
      z19=Y(IMF+K)+z19
      avden=avden+Y(IMF+K)
213   continue
      avcp=(z18+forcig*gamai*chwi/(gamai-1.)/tempi)/(z19+chwi)
      avden=(avden+chwi)/(volg+cov1)
      avvel=.5*y(1)
      htns=lambda*avcp*avden*avvel+ho
      z(5)=areaw*htns*(tgas-wallt)*hl
      elht=y(5)
      wallt=(elht+htfr*elbr)/cshl/rhocs/areaw/tshl+twal
c     write(3,*)lambda,avcp,avden,avvel,ho,areaw,htns,tgas,wallt,hl,z(5)
c    &,elht
c     ENERGY LOSS DUE TO AIR RESISTANCE
      air=iair
      z(8)=y(1)*pgas*air
      elar=areab*y(8)
c     RECOIL
      z(6)=0.0
      if(pbrch.le.rp(1)/areab)go to 221
      rfor=rp(2)
      if(y(3)-tr0.ge.tr(2))go to 222
      rfor=(tr(2)-(y(3)-tr0))/(tr(2)-tr(1))
      rfor=rp(2)-rfor*(rp(2)-rp(1))
```

```
222   z(6)=areab/rcwt*(pbrch-rfor/areab-resp)
      if(y(6).lt.0.0)y(6)=0.0
      z(7)=y(6)
      goto 223
221   tr0=y(3)
223   continue
c     CALCULATE GAS TEMPERATURE
      eprop=0.0
      rprop=0.0
      do 231 k=1,nprop
      eprop=eprop+forcp(k)*Y(IMF+K)/(gamap(k)-1.)
      rprop=rprop+forcp(k)*Y(IMF+K)/(gamap(k)-1.)/tempp(k)
231   continue
      tenergy=elpt+elpr+elgpm+elbr+elrc+elht+elar
      tgas=(eprop+forcig*chwi/(gamai-1.)-elpt-elpr-elgpm-elbr-elrc-elht
     &-elar)/(rprop+forcig*chwi/(gamai-1.)/tempi)
c     FIND FREE VOLUME
      v1=0.0
      cov1=0.0
      do 241 k=1,nprop
      v1=(CHWP(K)-Y(IMF+K))/RHOP(K)+V1
      cov1=cov1+covp(k)*Y(IMF+K)
241   continue
      fwr1=volgi+areab*(y(2)+y(7))-v1
      if(cov1.le.fwr1)go to 194
      write(3,193)
193   format(1x,'mass prop*covolume gt free volume')
      stop
194   volg=volgi+areab*(y(2)+y(7))-v1-cov1
c     CALCULATE MEAN PRESSURE
      r1=0.0
      do 251 k=1,nprop
      r1=r1+forcp(k)*Y(IMF+K)/tempp(k)
251   continue
      pmean=tgas/volg*(r1+forcig*chwi/tempi)
259   resp=resp+pgas*air
      if(igrad.le.1)go to 252
      if(isw1.ne.0)go to 253
      pbase=pmean
      pbrch=pmean
      if(pbase.gt.resp+1.)isw1=1
      go to 257
c     USE CHAMBRAGE PRESSURE GRADIENT EQUATION
253   j1zp=bint(1)+(bvol*pt+areab/2.*pt*pt)/areab
      j2zp=(bvol+areab*pt)**2/areab/areab
      j3zp=bint(3)+areab*bint(1)*pt+bvol*pt*pt/2.+areab*pt*pt*pt/6.
      a2t=-tmpi*areab*areab/prwt/vzp/vzp
      alf=1.-a2t*j1zp
      a1t=tmpi*areab*(areab*y(1)*y(1)/vzp+areab*resp/prwt)/vzp/vzp
      bt=-tmpi*y(1)*y(1)*areab*areab/2./vzp/vzp/vzp
      bata=-a1t*j1zp-bt*j2zp
      gamma=alf+a2t*j3zp/vzp
      delta=bata+a1t*j3zp/vzp+bt*j4zp/vzp
c     calculate base pressure
      pbase=(pmean-delta)/gamma
c     calculate breech pressure
      pbrch=alf*pbase+bata
      go to 254
c     USE LAGRANGE PRESSURE GRADIENT EQUATION
252   if(isw1.ne.0)go to 256
```

```
      if(pmean.lt.resp)resp=pmean
c     CALCULATE BASE PRESSURE
256   pbase=(pmean+tmpi*resp/3./prwt)/(1.+tmpi/3./prwt)
      if(pbase.gt.resp+1.)isw1=1
c     CALCULATE BREECH PESSURE
      pbrch=pbase+tmpi/2./prwt*(pbase-resp)
c     CALCULATE PROJECTILE ACCELERATION
254   z(1)=areab*(pbase-resp)/prwt
      if(z(1).lt.0.0)go to 257
      go to 258
257   if(isw1.eq.0)z(1)=0.0
258   if(y(1).lt.0.0)y(1)=0.0
      z(2)=y(1)
c     GET BURNING RATE
      do 264 m=1,nprop
      z(ibrp+m)=0.0
      if(ibo(m).eq.1) goto 264
      if (ipdb(m).eq.1)go to 266
      do 262 k=1,nbr(m)
      if(pmean.gt.pres(m,k))go to 262
      go to 263
262   continue
      k=nbr(m)
263   z(ibrp+m)=beta(m,k)*(pmean*1.e-6)**alpha(m,k)
      go to 264
266   do 267 k=1,nbrn(m)
      if(pmean.gt.presn(m,k))go to 267
      go to 268
267   continue
      k=nbrn(m)
268   z(ibrp+m)=betan(m,k)*(pmean*1.e-6)**alphan(m,k)
264   continue
      do 21 i=1,nde
      d(i)=(z(i)-b(j)*p(i))*a(j)
      y(i)=deltat*d(i)+y(i)
      p(i)=3.*d(i)-ak(j)*z(i)+p(i)
 21   continue
 11   continue
      t=t+deltat
      if(pmaxm.gt.pmean)go to 281
      pmaxm=pmean
      tpmaxm=y(3)
281   if(pmaxba.gt.pbase)go to 282
      pmaxba=pbase
      tpmaxba=y(3)
282   if(pmaxbr.gt.pbrch)go to 283
      pmaxbr=pbrch
      tpmaxbr=y(3)
283   continue
      if(y(3).lt.ptime)go to 272
      ptime=ptime+deltap
      write(3,7)y(3),z(1),y(1),y(2),pmean,pbase,pbrch
7     format(1x,7e11.4)
316   format(1x)
272   continue
      if(t.gt.tstop)goto 200
      if(y(2).gt.travp)go to 200
      rmvelo=y(1)
      tmvelo=y(3)
      disto=y(2)
```

```
      go to 19
200   write(3,311)t,y(3)
311   format(1x,' deltat t', e14.6, ' intg t',e14.6)
      write(3,312)pmaxm,tpmaxm
312   format(1x,'pmaxm Pa ',e14.6,' time at pmaxm sec ',e14.6)
      write(3,313)pmaxba,tpmaxba
313   format(1x,'pmaxba Pa ',e14.6,' time at pmaxba sec ',e14.6)
      write(3,314)pmaxbr,tpmaxbr
314   format(1x,'pmaxbr Pa ',e14.6,' time at pmaxbr sec ',e14.6)
      if(y(2).le.travp)go to 303
      dfract=(travp-disto)/(y(2)-disto)
      rmvel=(y(1)-rmvelo)*dfract+rmvelo
      tmvel=(y(3)-tmvelo)*dfract+tmvelo
      write(3,318)rmvel,tmvel
318   format(1x,'muzzle velocity m/s ',e14.6,' time of muzzle velocity s
     &ec ',e14.6)
      goto 319
303   write(3,327)y(1),y(3)
327   format(1x,'velocity of projectile m/s ',e14.6,' at this time msec
     &',e14.6)
319   efi=chwi*forcig/(gamai-1.)
      efp=0.0
      do 315 i=1,nprop
      efp=efp+chwp(i)*forcp(i)/(gamap(i)-1.0)
315   continue
      tenerg=efi+efp
      write(3,317)tenerg
317   format(1x,'total initial energy available J = ',e14.6)
      tengas=chwi*forcig*tgas/(gamai-1.)/tempi
      do 135 i=1,nprop
      tengas=(Y(IMF+I)*forcp(i)*tgas/tempp(i)/(gamap(i)-1.))+teng
     &as
      write(3,137)i,frac(i),tbo(i)
137   format(' FOR PROPELLANT ',i2,' MASS FRAC BURNT IS',e14.6,' AT TIME
     & ',e14.6)
135   continue
      write(3,136)tengas
136   format(1x,'total energy remaining in gas J= ',e14.6)
      write(3,320)elpt
320   format(1x,'energy loss from projectile translation J= ',e14.6)
      write(3,321)elpr
321   format(1x,'energy loss from projectile rotation J= ',e14.6)
      write(3,322)elgpm
322   format(1x,'energy lost to gas and propellant motion J= ',e14.6)
      write(3,323)elbr
323   format(1x,'energy lost to bore resistance J= ',e14.6)
      write(3,324)elrc
324   format(1x,'energy lost to recoil J= ',e14.6)
      write(3,325)elht
325   format(1x,'energy loss from heat transfer J= ',e14.6)
      write(3,326)elar
326   format(1x,'energy lost to air resistance J= ',e14.6)
c     call gettim(ihro,imino,iseco,ihunso)
c     time=(ihro-ihr)*3600.+(imino-imin)*60.+(iseco-isec)+(ihunso-ihuns)
c    &/100.
c     write(3,*)time
      stop
 20   write(*,140)
140   format(1x,'end of file encounter')
      stop
```

```
 30   write(*,150)
999   continue
998   continue
150   format(1x,'read or write error')
      stop
      end
      SUBROUTINE PRF017(P,P1,D,D1,L,SURF,MASSF,X,NP,u)
      IMPLICIT REAL*4(A-Z)
C
C     P=OUTER PERF DIA
C     P1=INNER PERF DIA
C     D=OUTER DIA
C     D1=DISTANCE BETWEEN PERF CENTRES
C     L=GRAIN LENGTH
C     NP=NUMBER OF PERFS
C
C     SURF=OUTPUT SURFACE AREA
C     MASSF=OUTPUT MASS FRACTION OF PROPELLANT BURNER
C
C     W=WEB BETWEEN OUTER PERFS
C     W0=OUTER WEB
C     W1=WEB BETWEEN OUTER AND INNER PERFS
C     W4=MINIMUM WEB
C     U=INITIAL VOLUME OF 1 GRAIN
C
      INTEGER ITYM,NP
      DATA PI,SQRT3/3.141592654,1.732050808/,ITYM/0/
      DATA HAFPI,PIFOR,TWOPI/1.570796327,.785398164,6.283185308/
C
      IF(ITYM.GT.0)GO TO 10
      P1SQ=P1*P1
      D1SQ=D1*D1
      PSQ=P*P
      DSQ=D*D
      D1SQ3=D1*SQRT3
      D2SQ3=D1SQ*SQRT3
      IF(NP.EQ.0)GO TO 2000
      IF(NP.EQ.1)GO TO 3000
      IF(NP.NE.7)GO TO 60
      IF(P1.GT.(P+D1*(SQRT3-1))) GO TO 60
      IF(D.GE.D1*(SQRT3+1.)-P)GO TO 130
 60   WRITE(6,90)
 90   FORMAT(1X,'UNACCEPTABLE GRANULATION')
      STOP
130   W=D1-P
      IF(W.LT.0)GO TO 60
      W0=(D-P-2.*D1)/2.
      IF(W0.LT.0.)GO TO 60
      W1=(2.*D1-P-P1)/2.
      IF(W1.LT.0.)GO TO 60
      X1=(P1SQ-PSQ+4.*D1SQ-2.*P1*D1SQ3)/4./(D1SQ3+P-P1)
      X2=(4.*D1SQ+D*D-2.*D*D1SQ3-PSQ)/4./(-D1SQ3+P+D)
      A=PI*L*(D+P1+6.*P)+HAFPI*(DSQ-P1SQ-6.*PSQ)
      U=PI*L/4.*(DSQ-P1SQ-6.*PSQ)
      W4=AMIN1(W,W0,W1)
 10   MASSF=0.
      TWOX=X+X
      XSQ=X*X
      P1P2X=P1+TWOX
      PP2X=P+TWOX
```

```
      DM2X=D-TWOX
      LM2X=L-TWOX
      P12XSQ=P1P2X*P1P2X
      PP2XSQ=PP2X*PP2X
      DM2XSQ=DM2X*DM2X
      IF(NP.EQ.0)GO TO 2000
      IF(NP.EQ.1)GO TO 3000
      IF(LM2X.GT.0)GO TO 340
      SURF=0.
      V=0.
      GO TO 850
  340 S0=PI*LM2X*(D+P1+6.*P+12.*X)+HAFPI*(DM2X*DM2X
     1 -P1P2X*P1P2X-6.*PP2X*PP2X)
      V0=PIFOR*LM2X*(DM2X*DM2X-P1P2X*P1P2X-6.*PP2X*PP2X)
      IF(X.GT.W4/2.)GO TO 360
      MASSF=-TWOX/L/(DSQ-P1SQ-6.*PSQ)
      MASSF=MASSF*(24.*XSQ+(24.*P+4.*P1+4.*D-12.*L)*X+P1SQ
     1 +6.*PSQ-2.*L*D-2.*P1*L-12.*L*P-DSQ)
      SURF=S0
      RETURN
  360 IF(X.GT.W '2.)GO TO 390
      F2=0.
      L2=0.
      A3=0.
      A4=0.
      GO TO 460
  390 Z=(2.*D1+P+P1+4.*X)/4.
      B3=((P1-P)*(P1+P+4.*X)+4.*D1SQ)/4./D1/P1P2X
      A3=ATAN(SQRT(1.-B3*B3)/B3)
      B4=((P-P1)*(P+P1+4.*X)+4.*D1SQ)/4./D1/PP2X
      A4=ATAN(SQRT(1.-B4*B4)/B4)
      F2=A3/4.*P12XSQ+A4/4.*PP2XSQ
     1 -SQRT(Z*(Z-D1)*(2.*Z-P-TWOX)*(2.*Z-P1-TWOX))
      L2=LM2X*(A4*PP2X+A3*P1P2X)
  460 IF(X.GT.W/2.)GO TO 490
      F3=0.
      L3=0.
      A5=0.
      GO TO 530
  490 B5=D1/PP2X
      A5=ATAN(SQRT(1.-B5*B5)/B5)
      F3=(A5*PP2XSQ-D1*SQRT(PP2XSQ-D1SQ))/2.
      L3=2.*A5*LM2X*PP2X
  530 IF(X.GT.W0/2.)GO TO 560
      F1=0.
      L1=0.
      A1=0.
      A2=0.
      GO TO 650
  560 Y=(2.*D1+P+D)/4.
      B1=((D+P)*(D-P-4.*X)-4.*D1SQ)/4./D1/PP2X
      A1=ATAN(SQRT(1.-B1*B1)/B1)
      IF(A1.GT.0.)GO TO 610
      A1=PI+A1
  610 B2=((D+P)*(D-P-4.*X)+4.*D1SQ)/4./D1/DM2X
      A2=ATAN(SQRT(1.-B2*B2)/B2)
      F1=A1/4.*PP2XSQ-A2/4.*DM2XSQ+SQRT(Y*(Y-D1)
     1 *(2.*Y-P-TWOX)*(2.*Y-D+TWOX))
      L1=LM2X*(A1*PP2X+A2*DM2X)
  650 IF(X.GT.W/2.)GO TO 690
```

```
      SURF=S0+12.*(F1+F2+F3)-6.*(L1+L2+L3)
      V=V0+6.*(F1+F2+F3)*LM2X
      GO TO 850
  690 IF(X.LT.X1)GO TO 730
      S1=0.0
      V1=0.0
      GO TO 760
  730 S1=3.*D2SQ3-PI*PP2XSQ-HAFPI*P12XSQ
     $ +6.*F3+12.*F2
      S1=S1+LM2X*(2.*(PI-3.*A5-3.*A4)*PP2X+(PI-6.*A3)
     $ *P1P2X)
      V1=LM2X/2.*(3.*D2SQ3-PI*PP2XSQ
     $ -HAFPI*P12XSQ+6.*F3+12.*F2)
  760 IF(X.LT.X2) GO TO 800
      S2=0.0
      V2=0.0
      GO TO 830
  800 S2=HAFPI*DM2XSQ-3.*D2SQ3-TWOPI*PP2XSQ
     $ +12.*F1+6.*F3
      S2=S2+LM2X*((PI-6.*A2)*DM2X+2.*(TWOPI-3.*A1-3.*A5)
     $ *PP2X)
      V2=LM2X/2.*(HAFPI*DM2XSQ-3.*D2SQ3-TWOPI
     $ *PP2XSQ+12.*F1+6.*F3)
  830 SURF=S1+S2
      V=V1+V2
  850 MASSF=1.-V/U
      RETURN
C
C ZERO PERF CALCULATIONS START HERE.
C
 2000 if(d-2*x.le.0.0) go to 2001
      twox=x+x
      xsq=x*x
      MASSF=TWOX*(DSQ+2.*L*D-4.*X*D-TWOX*L+4.*XSQ)/(DSQ*L)
      u=dsq*l*pi/4.
      SURF=PI*(DSQ/2.-4.*D*X-TWOX*L+D*L+6.*XSQ)
      RETURN
2001  surf=0.0
      massf=1.0
      u=dsq*l*pi/4.
      return
C
C ONE PERF CALCULATIONS START HERE.
C
 3000 if(d-p-4.*x.le.0.0) goto 3001
      twox=x+x
      MASSF=TWOX*(DSQ+2.*L*D-4.*X*D-PSQ+2.*P*L-4.*P*X)
     $ /(DSQ*L-PSQ*L)
      u=dsq*l*pi/4.-psq*l*pi/4.
      SURF=PI*(DSQ/2.-4.*D*X-4.*X*P+D*L+P*L-PSQ/2.)
      RETURN
3001  surf=0.0
      massf=1.0
      u=dsq*l*pi/4.-psq*l*pi/4.
      return
      END
      SUBROUTINE MONO(PD,GD,GL,SURF,FRAC,X,VOL0)
      DATA ITYM/0/,PI/3.141592654/
C
C PD = PERF DIAMETER
```

```
C GD = GRAIN DIAMETER
C GL = GRAIN LENGTH
C SURF = INSTANTANEOUS SURFACE AREA
C FRAC = MASS FRACTION BURNT
C VOL = INSTANTANEOUS VOLUME REMAINING
C X = DEPTH BURNT
C VOL0 = INITIAL VOLUME
C ASSUMES END AND LATERAL SURFACES UNLIMITED
C
      VOL0=PI*(GD*GD/4.-PD*PD/4.)*GL
      SURF=PI*PD*GL
      FRAC=0.0
      IF(ITYM.NE.0)GO TO 10
      ITYM=1
      RETURN
10    IF(X.GE.(GD-PD)/2.)GO TO 20
      IF(X.GE.GL/2.)GO TO 20
      VOL=PI*(GD*GD/4.-(PD+2.*X)**2/4.)*GL
      FRAC=1.-VOL/VOL0
      SURF=PI*(PD+2.*X)*GL
      RETURN
C     BURNOUT
20    FRAC=1.0
      SURF=0.0
      RETURN
      END
C
      SUBROUTINE CIG(GD,GL,SURF,FRAC,X,VOL0)
      DATA ITYM/0/,PI/3.141592654/
C
C GD = GRAIN DIAMETER
C GL = GRAIN LENGTH
C SURF = INSTANTANEOUS SURF (CONSTANT)
C VOL = INSTANTANEOUS VOLUME REMAINING
C FRAC = FRACTION OF PROPELLENT BURNT
C X = DEPTH BURNT
C VOL0 = INITIAL VOLUME
C
C ASSUMES BURNS ON ONE END SURFACE ONLY
C
      VOL0=PI*GD*GD/4.*GL
      SURF=PI*GD*GD/4.
      FRAC=0.0
      IF(ITYM.NE.0)GO TO 10
      ITYM=1
      RETURN
10    IF(X.GE.GL)GO TO 20
      VOL=PI*GD*GD/4.*(GL-X)
      FRAC=1.-VOL/VOL0
      RETURN
C BURNOUT
20    FRAC=1.0
      SURF=0.0
      RETURN
      END
```

APPENDIX B
Listing of Input Data
IBM1

INTENTIONALLY LEFT BLANK.

```
   9832.2384 12.7 12.7 1.0 0.0  457.2 1
   9.796 0 0.0 0.0
5  0.0 0.0 0.0 .6 0.0 1.3 0.0 300. 0. 457.
   1.e20 2 3.0e+4 0.0 8.0e+5 0.2
   .001135 .01143 .46028 273. 1. 7.8612
   84.5535 .9755 294. .004712 1.4
1
1  1160. 3141. 1.12 11.3557 1.53 1.23 -1 50. 0. 9.36 15. .0 1
   0.0 .1 7. 0.
   1 1.0 2.69 689.476
   1 1.0 2.69 689.476
   .005 .05 30.
```

INTENTIONALLY LEFT BLANK.

APPENDIX C
Listing of Output

INTENTIONALLY LEFT BLANK.

```
 USING INPUT FILE ibm1
using Lagrange pressure gradient
chamber volume cm**3  0.983224E+04
 groove diam cm  0.127000E+02
land diam cm  0.127000E+02
 groove/land ratio  0.100000E+01
 twist turns/caliber  0.000000E+00
 projectile travel cm  0.457200E+03



projectile mass kg  0.979600E+01
 switch to calculate energy lost to air resistance J 0
 fraction of work against bore used to heat the tube  0.000000E+00
 gas pressure Pa  0.000000E+00
number barrel resistance points 5
 bore resistance MPa - travel cm
  0.000000E+00  0.000000E+00
  0.000000E+00  0.600000E+00
  0.000000E+00  0.130000E+01
  0.000000E+00  0.300000E+03
  0.000000E+00  0.457000E+03

  mass of recoiling parts kg  0.100000E+21
 number of recoil point pairs 2
 recoil force N  recoil time sec
  0.300000E+05      0.000000E+00
  0.800000E+06      0.200000E+00

  free convective heat transfer coefficient w/cm**2 k  0.113500E-02
 chamber wall thickness cm  0.114300E-01
 heat capacity of steel of chamber wall j/g k  0.460280E+00
 initial temperature of chamber wall k  0.273000E+03
 heat loss coefficient  0.100000E+01
 density of chamber wall steel g/cm**3  0.786120E+01


  impetus of igniter propellant J/g  0.845535E+02
 covolume of igniter cm**3/g  0.975500E+00
 adiabatic flame temperature of igniter propellant k  0.294000E+03
 initial mass of igniter kg  0.471200E-02
ratio of specific heats for igniter  0.140000E+01


for propellant number  1
 impetus of propellant J/g  0.116000E+04
 adiabatic temperature of propellant K  0.314100E+04
 covolume of propellant cm**3/g  0.112000E+01
 initial mass of propellant kg  0.113557E+02
 density of propellant g/cm**3  0.153000E+01
 ratio of specific heats for propellant  0.123000E+01
 number of perforations of propellant-1
 length of propellant grain cm  0.500000E+02
 diameter of inner perforation in propellant grains cm  0.000000E+00
 diameter of outerperforation of propellant grains cm  0.936000E+01
 outside diameter of propellant grain cm  0.150000E+02
 distance between perf centers cm  0.000000E+00
```

```
propellant wt changed to    0.825482E+01 kg
IN DEPTH BURNING WILL OCCUR WHEN TIME IS GREATER THAN    0.000000E+00 MSEC
 AND PRESSURE IS GREATER THAN    0.100000E+00MPa
INITIAL DEPTH BURNT PENETRATION mm    0.700000E+01
AND INITIAL SURFACE AREA/UNIT VOLUME m**2/m**3    0.000000E+00

the calculated number of grains for propellant  1 is    0.100000E+01
 for propellant  1 the number of burning rate points is 1
    exponent          coefficient              pressure
    -                cm/sec-mpa**ai            mpa
  0.100000E+01        0.269000E+01                  0.689476E+03
THE INTERIOR BURNING SURFACE FOR IN-DEPTH BURNING WILL REGRESS ACCORDING TO
number of burning rate points 1
    exponent          coefficient              pressure
    -                cm/sec-mpa**ai            mpa
  0.100000E+01        0.269000E+01                  0.689476E+03

time increment msec  0.500000E-02  print increment msec  0.500000E-01
time to stop calculation msec    0.300000E+02
area bore m^2      0.126677E-01 pressure from ign pa     0.898886E+05
 volume of unburnt prop m^3      0.539531E-02 init cham vol-cov ign m ^3      0.9
   time        acc          vel          dis          mpress      pbase       pbrch
 0.5000E-05 0.9194E+02 0.4557E-03 0.1137E-08 0.9108E+05 0.7110E+05 0.1011E+06
 0.5500E-04 0.1046E+03 0.5358E-02 0.1438E-06 0.1036E+06 0.8089E+05 0.1150E+06
 0.1050E-03 0.1191E+03 0.1094E-01 0.5483E-06 0.1180E+06 0.9209E+05 0.1309E+06
 0.1550E-03 0.1354E+03 0.1730E-01 0.1251E-05 0.1341E+06 0.1047E+06 0.1488E+06
 0.2050E-03 0.1536E+03 0.2451E-01 0.2292E-05 0.1521E+06 0.1188E+06 0.1688E+06
 0.2550E-03 0.1739E+03 0.3269E-01 0.3718E-05 0.1723E+06 0.1345E+06 0.1912E+06
 0.3050E-03 0.1966E+03 0.4194E-01 0.5579E-05 0.1947E+06 0.1520E+06 0.2161E+06
 0.3550E-03 0.2217E+03 0.5238E-01 0.7932E-05 0.2196E+06 0.1714E+06 0.2437E+06
 0.4050E-03 0.2495E+03 0.6415E-01 0.1084E-04 0.2471E+06 0.1929E+06 0.2742E+06
 0.4550E-03 0.2801E+03 0.7737E-01 0.1437E-04 0.2775E+06 0.2166E+06 0.3079E+06
 0.5050E-03 0.3138E+03 0.9221E-01 0.1860E-04 0.3108E+06 0.2426E+06 0.3449E+06
 0.5550E-03 0.3506E+03 0.1088E+00 0.2362E-04 0.3474E+06 0.2712E+06 0.3855E+06
 0.6050E-03 0.3909E+03 0.1273E+00 0.2952E-04 0.3873E+06 0.3023E+06 0.4298E+06
 0.6550E-03 0.4349E+03 0.1480E+00 0.3639E-04 0.4308E+06 0.3363E+06 0.4781E+06
 0.7050E-03 0.4826E+03 0.1709E+00 0.4435E-04 0.4781E+06 0.3732E+06 0.5306E+06
 0.7550E-03 0.5344E+03 0.1963E+00 0.5352E-04 0.5294E+06 0.4133E+06 0.5875E+06
 0.8050E-03 0.5906E+03 0.2244E+00 0.6402E-04 0.5850E+06 0.4567E+06 0.6492E+06
 0.8550E-03 0.6513E+03 0.2554E+00 0.7601E-04 0.6452E+06 0.5036E+06 0.7159E+06
 0.9050E-03 0.7168E+03 0.2896E+00 0.8962E-04 0.7101E+06 0.5543E+06 0.7880E+06
 0.9550E-03 0.7876E+03 0.3272E+00 0.1050E-03 0.7802E+06 0.6090E+06 0.8658E+06
 0.1005E-02 0.8639E+03 0.3684E+00 0.1224E-03 0.8558E+06 0.6681E+06 0.9497E+06
 0.1055E-02 0.9462E+03 0.4137E+00 0.1419E-03 0.9373E+06 0.7317E+06 0.1040E+07
 0.1105E-02 0.1035E+04 0.4632E+00 0.1638E-03 0.1025E+07 0.8002E+06 0.1138E+07
 0.1155E-02 0.1130E+04 0.5173E+00 0.1883E-03 0.1120E+07 0.8741E+06 0.1243E+07
 0.1205E-02 0.1233E+04 0.5763E+00 0.2156E-03 0.1222E+07 0.9537E+06 0.1356E+07
 0.1255E-02 0.1344E+04 0.6407E+00 0.2460E-03 0.1332E+07 0.1040E+07 0.1478E+07
 0.1305E-02 0.1464E+04 0.7109E+00 0.2798E-03 0.1450E+07 0.1132E+07 0.1609E+07
 0.1355E-02 0.1593E+04 0.7873E+00 0.3172E-03 0.1578E+07 0.1232E+07 0.1751E+07
 0.1405E-02 0.1732E+04 0.8703E+00 0.3586E-03 0.1716E+07 0.1339E+07 0.1904E+07
 0.1455E-02 0.1882E+04 0.9606E+00 0.4044E-03 0.1864E+07 0.1455E+07 0.2069E+07
 0.1505E-02 0.2044E+04 0.1059E+01 0.4548E-03 0.2025E+07 0.1581E+07 0.2247E+07
 0.1555E-02 0.2219E+04 0.1165E+01 0.5104E-03 0.2198E+07 0.1716E+07 0.2439E+07
 0.1605E-02 0.2407E+04 0.1281E+01 0.5715E-03 0.2385E+07 0.1861E+07 0.2646E+07
 0.1655E-02 0.2611E+04 0.1406E+01 0.6386E-03 0.2586E+07 0.2019E+07 0.2870E+07
 0.1705E-02 0.2831E+04 0.1542E+01 0.7123E-03 0.2804E+07 0.2189E+07 0.3112E+07
 0.1755E-02 0.3068E+04 0.1690E+01 0.7930E-03 0.3039E+07 0.2373E+07 0.3373E+07
 0.1805E-02 0.3325E+04 0.1849E+01 0.8815E-03 0.3294E+07 0.2571E+07 0.3655E+07
 0.1855E-02 0.3602E+04 0.2022E+01 0.9782E-03 0.3568E+07 0.2785E+07 0.3960E+07
```

0.1905E-02	0.3901E+04	0.2210E+01	0.1084E-02	0.3865E+07	0.3017E+07	0.4289E+07
0.1955E-02	0.4225E+04	0.2413E+01	0.1199E-02	0.4185E+07	0.3267E+07	0.4645E+07
0.2005E-02	0.4575E+04	0.2633E+01	0.1326E-02	0.4532E+07	0.3538E+07	0.5029E+07
0.2055E-02	0.4953E+04	0.2871E+01	0.1463E-02	0.4906E+07	0.3830E+07	0.5444E+07
0.2105E-02	0.5361E+04	0.3128E+01	0.1613E-02	0.5311E+07	0.4146E+07	0.5893E+07
0.2155E-02	0.5802E+04	0.3407E+01	0.1776E-02	0.5748E+07	0.4487E+07	0.6378E+07
0.2205E-02	0.6279E+04	0.3709E+01	0.1954E-02	0.6220E+07	0.4856E+07	0.6903E+07
0.2255E-02	0.6794E+04	0.4036E+01	0.2148E-02	0.6731E+07	0.5254E+07	0.7469E+07
0.2305E-02	0.7351E+04	0.4389E+01	0.2358E-02	0.7282E+07	0.5685E+07	0.8081E+07
0.2355E-02	0.7953E+04	0.4772E+01	0.2587E-02	0.7878E+07	0.6150E+07	0.8742E+07
0.2405E-02	0.8602E+04	0.5185E+01	0.2836E-02	0.8522E+07	0.6652E+07	0.9457E+07
0.2455E-02	0.9304E+04	0.5633E+01	0.3106E-02	0.9217E+07	0.7195E+07	0.1023E+08
0.2505E-02	0.1006E+05	0.6117E+01	0.3400E-02	0.9968E+07	0.7781E+07	0.1106E+08
0.2555E-02	0.1088E+05	0.6640E+01	0.3718E-02	0.1078E+08	0.8414E+07	0.1196E+08
0.2605E-02	0.1176E+05	0.7206E+01	0.4064E-02	0.1165E+08	0.9098E+07	0.1293E+08
0.2655E-02	0.1272E+05	0.7818E+01	0.4440E-02	0.1260E+08	0.9836E+07	0.1398E+08
0.2705E-02	0.1375E+05	0.8479E+01	0.4847E-02	0.1362E+08	0.1063E+08	0.1511E+08
0.2755E-02	0.1486E+05	0.9194E+01	0.5289E-02	0.1472E+08	0.1149E+08	0.1634E+08
0.2805E-02	0.1606E+05	0.9966E+01	0.5767E-02	0.1591E+08	0.1242E+08	0.1765E+08
0.2855E-02	0.1735E+05	0.1080E+02	0.6286E-02	0.1719E+08	0.1342E+08	0.1907E+08
0.2905E-02	0.1875E+05	0.1170E+02	0.6849E-02	0.1857E+08	0.1450E+08	0.2061E+08
0.2955E-02	0.2025E+05	0.1268E+02	0.7458E-02	0.2006E+08	0.1566E+08	0.2226E+08
0.3005E-02	0.2187E+05	0.1373E+02	0.8118E-02	0.2166E+08	0.1691E+08	0.2404E+08
0.3055E-02	0.2361E+05	0.1487E+02	0.8832E-02	0.2339E+08	0.1826E+08	0.2596E+08
0.3105E-02	0.2549E+05	0.1609E+02	0.9606E-02	0.2525E+08	0.1971E+08	0.2802E+08
0.3155E-02	0.2751E+05	0.1742E+02	0.1044E-01	0.2725E+08	0.2127E+08	0.3024E+08
0.3205E-02	0.2968E+05	0.1885E+02	0.1135E-01	0.2940E+08	0.2295E+08	0.3263E+08
0.3255E-02	0.3202E+05	0.2039E+02	0.1233E-01	0.3172E+08	0.2476E+08	0.3520E+08
0.3305E-02	0.3453E+05	0.2205E+02	0.1339E-01	0.3421E+08	0.2670E+08	0.3796E+08
0.3355E-02	0.3723E+05	0.2384E+02	0.1454E-01	0.3688E+08	0.2879E+08	0.4092E+08
0.3405E-02	0.4012E+05	0.2578E+02	0.1578E-01	0.3975E+08	0.3103E+08	0.4411E+08
0.3455E-02	0.4322E+05	0.2786E+02	0.1712E-01	0.4282E+08	0.3343E+08	0.4752E+08
0.3505E-02	0.4655E+05	0.3010E+02	0.1857E-01	0.4612E+08	0.3600E+08	0.5117E+08
0.3555E-02	0.5011E+05	0.3252E+02	0.2013E-01	0.4965E+08	0.3875E+08	0.5509E+08
0.3605E-02	0.5393E+05	0.3512E+02	0.2182E-01	0.5342E+08	0.4170E+08	0.5928E+08
0.3655E-02	0.5800E+05	0.3792E+02	0.2365E-01	0.5746E+08	0.4485E+08	0.6376E+08
0.3705E-02	0.6235E+05	0.4092E+02	0.2562E-01	0.6177E+08	0.4822E+08	0.6855E+08
0.3755E-02	0.6700E+05	0.4416E+02	0.2774E-01	0.6637E+08	0.5181E+08	0.7365E+08
0.3805E-02	0.7195E+05	0.4763E+02	0.3003E-01	0.7127E+08	0.5564E+08	0.7909E+08
0.3855E-02	0.7721E+05	0.5136E+02	0.3251E-01	0.7649E+08	0.5971E+08	0.8488E+08
0.3905E-02	0.8281E+05	0.5535E+02	0.3518E-01	0.8204E+08	0.6404E+08	0.9104E+08
0.3955E-02	0.8876E+05	0.5964E+02	0.3805E-01	0.8793E+08	0.6864E+08	0.9757E+08
0.4005E-02	0.9506E+05	0.6424E+02	0.4114E-01	0.9417E+08	0.7351E+08	0.1045E+09
0.4055E-02	0.1017E+06	0.6915E+02	0.4448E-01	0.1008E+09	0.7866E+08	0.1118E+09
0.4105E-02	0.1088E+06	0.7441E+02	0.4807E-01	0.1078E+09	0.8411E+08	0.1196E+09
0.4155E-02	0.1162E+06	0.8004E+02	0.5193E-01	0.1151E+09	0.8986E+08	0.1277E+09
0.4205E-02	0.1240E+06	0.8604E+02	0.5608E-01	0.1229E+09	0.9590E+08	0.1363E+09
0.4255E-02	0.1322E+06	0.9245E+02	0.6054E-01	0.1310E+09	0.1023E+09	0.1454E+09
0.4305E-02	0.1408E+06	0.9927E+02	0.6533E-01	0.1395E+09	0.1089E+09	0.1548E+09
0.4355E-02	0.1499E+06	0.1065E+03	0.7047E-01	0.1484E+09	0.1159E+09	0.1647E+09
0.4405E-02	0.1592E+06	0.1143E+03	0.7599E-01	0.1578E+09	0.1231E+09	0.1751E+09
0.4455E-02	0.1690E+06	0.1225E+03	0.8190E-01	0.1674E+09	0.1307E+09	0.1858E+09
0.4505E-02	0.1793E+06	0.1312E+03	0.8824E-01	0.1775E+09	0.1386E+09	0.1970E+09
0.4555E-02	0.1897E+06	0.1404E+03	0.9503E-01	0.1879E+09	0.1467E+09	0.2085E+09
0.4605E-02	0.2005E+06	0.1501E+03	0.1023E+00	0.1986E+09	0.1551E+09	0.2204E+09
0.4655E-02	0.2117E+06	0.1604E+03	0.1101E+00	0.2097E+09	0.1637E+09	0.2327E+09
0.4705E-02	0.2231E+06	0.1713E+03	0.1183E+00	0.2210E+09	0.1725E+09	0.2452E+09
0.4755E-02	0.2347E+06	0.1828E+03	0.1272E+00	0.2326E+09	0.1815E+09	0.2581E+09
0.4805E-02	0.2466E+06	0.1948E+03	0.1366E+00	0.2443E+09	0.1907E+09	0.2711E+09
0.4855E-02	0.2587E+06	0.2074E+03	0.1467E+00	0.2562E+09	0.2000E+09	0.2844E+09

0.4905E-02	0.2708E+06	0.2207E+03	0.1574E+00	0.2683E+09	0.2094E+09	0.2977E+09
0.4955E-02	0.2831E+06	0.2345E+03	0.1688E+00	0.2804E+09	0.2189E+09	0.3112E+09
0.5005E-02	0.2953E+06	0.2490E+03	0.1808E+00	0.2925E+09	0.2284E+09	0.3246E+09
0.5055E-02	0.3075E+06	0.2640E+03	0.1937E+00	0.3046E+09	0.2378E+09	0.3380E+09
0.5105E-02	0.3196E+06	0.2797E+03	0.2073E+00	0.3166E+09	0.2472E+09	0.3513E+09
0.5155E-02	0.3316E+06	0.2960E+03	0.2216E+00	0.3285E+09	0.2564E+09	0.3645E+09
0.5205E-02	0.3433E+06	0.3129E+03	0.2369E+00	0.3401E+09	0.2655E+09	0.3774E+09
0.5255E-02	0.3547E+06	0.3303E+03	0.2529E+00	0.3514E+09	0.2743E+09	0.3900E+09
0.5305E-02	0.3659E+06	0.3483E+03	0.2699E+00	0.3624E+09	0.2829E+09	0.4022E+09
0.5355E-02	0.3766E+06	0.3669E+03	0.2878E+00	0.3731E+09	0.2912E+09	0.4140E+09
0.5405E-02	0.3869E+06	0.3860E+03	0.3066E+00	0.3833E+09	0.2992E+09	0.4253E+09
0.5455E-02	0.3967E+06	0.4056E+03	0.3264E+00	0.3930E+09	0.3068E+09	0.4361E+09
0.5505E-02	0.4060E+06	0.4256E+03	0.3472E+00	0.4022E+09	0.3140E+09	0.4464E+09
0.5555E-02	0.4148E+06	0.4462E+03	0.3690E+00	0.4109E+09	0.3207E+09	0.4560E+09
0.5605E-02	0.4229E+06	0.4671E+03	0.3918E+00	0.4189E+09	0.3270E+09	0.4649E+09
0.5655E-02	0.4304E+06	0.4885E+03	0.4157E+00	0.4264E+09	0.3328E+09	0.4732E+09
0.5705E-02	0.4373E+06	0.5101E+03	0.4406E+00	0.4332E+09	0.3382E+09	0.4807E+09
0.5755E-02	0.4435E+06	0.5322E+03	0.4667E+00	0.4393E+09	0.3430E+09	0.4875E+09
0.5805E-02	0.4490E+06	0.5545E+03	0.4939E+00	0.4448E+09	0.3472E+09	0.4936E+09
0.5855E-02	0.4539E+06	0.5771E+03	0.5222E+00	0.4497E+09	0.3510E+09	0.4990E+09
0.5905E-02	0.4581E+06	0.5999E+03	0.5516E+00	0.4539E+09	0.3543E+09	0.5036E+09
0.5955E-02	0.4617E+06	0.6229E+03	0.5821E+00	0.4574E+09	0.3570E+09	0.5076E+09
0.6005E-02	0.4646E+06	0.6460E+03	0.6139E+00	0.4603E+09	0.3593E+09	0.5108E+09
0.6055E-02	0.4669E+06	0.6693E+03	0.6467E+00	0.4625E+09	0.3611E+09	0.5133E+09
0.6105E-02	0.4686E+06	0.6927E+03	0.6808E+00	0.4642E+09	0.3624E+09	0.5151E+09
0.6155E-02	0.4697E+06	0.7162E+03	0.7160E+00	0.4653E+09	0.3632E+09	0.5163E+09
0.6205E-02	0.4702E+06	0.7397E+03	0.7524E+00	0.4658E+09	0.3636E+09	0.5169E+09
0.6255E-02	0.4702E+06	0.7632E+03	0.7900E+00	0.4658E+09	0.3636E+09	0.5169E+09
0.6305E-02	0.4697E+06	0.7867E+03	0.8287E+00	0.4653E+09	0.3632E+09	0.5164E+09
0.6355E-02	0.4688E+06	0.8101E+03	0.8687E+00	0.4644E+09	0.3625E+09	0.5153E+09
0.6405E-02	0.4674E+06	0.8335E+03	0.9097E+00	0.4630E+09	0.3614E+09	0.5138E+09
0.6455E-02	0.4656E+06	0.8569E+03	0.9520E+00	0.4612E+09	0.3600E+09	0.5118E+09
0.6505E-02	0.4634E+06	0.8801E+03	0.9954E+00	0.4591E+09	0.3583E+09	0.5094E+09
0.6555E-02	0.4609E+06	0.9032E+03	0.1040E+01	0.4566E+09	0.3564E+09	0.5066E+09
0.6605E-02	0.4580E+06	0.9262E+03	0.1086E+01	0.4537E+09	0.3542E+09	0.5035E+09
0.6655E-02	0.4549E+06	0.9490E+03	0.1133E+01	0.4506E+09	0.3518E+09	0.5001E+09
0.6705E-02	0.4515E+06	0.9717E+03	0.1181E+01	0.4473E+09	0.3492E+09	0.4964E+09
0.6755E-02	0.4479E+06	0.9942E+03	0.1230E+01	0.4437E+09	0.3464E+09	0.4924E+09
0.6805E-02	0.4441E+06	0.1016E+04	0.1280E+01	0.4399E+09	0.3434E+09	0.4882E+09
0.6855E-02	0.4401E+06	0.1039E+04	0.1331E+01	0.4360E+09	0.3403E+09	0.4838E+09
0.6905E-02	0.4343E+06	0.1060E+04	0.1384E+01	0.4303E+09	0.3359E+09	0.4775E+09
0.6955E-02	0.4152E+06	0.1082E+04	0.1437E+01	0.4113E+09	0.3210E+09	0.4564E+09
0.7005E-02	0.3969E+06	0.1102E+04	0.1492E+01	0.3932E+09	0.3069E+09	0.4363E+09
0.7055E-02	0.3797E+06	0.1121E+04	0.1548E+01	0.3762E+09	0.2937E+09	0.4175E+09
0.7105E-02	0.3636E+06	0.1140E+04	0.1604E+01	0.3602E+09	0.2812E+09	0.3997E+09
0.7155E-02	0.3485E+06	0.1158E+04	0.1662E+01	0.3452E+09	0.2695E+09	0.3831E+09
0.7205E-02	0.3342E+06	0.1175E+04	0.1720E+01	0.3311E+09	0.2585E+09	0.3674E+09
0.7255E-02	0.3208E+06	0.1191E+04	0.1779E+01	0.3178E+09	0.2481E+09	0.3527E+09
0.7305E-02	0.3082E+06	0.1207E+04	0.1839E+01	0.3053E+09	0.2383E+09	0.3388E+09
0.7355E-02	0.2962E+06	0.1222E+04	0.1900E+01	0.2935E+09	0.2291E+09	0.3257E+09
0.7405E-02	0.2850E+06	0.1237E+04	0.1961E+01	0.2823E+09	0.2204E+09	0.3133E+09
0.7455E-02	0.2744E+06	0.1251E+04	0.2023E+01	0.2718E+09	0.2122E+09	0.3016E+09
0.7505E-02	0.2643E+06	0.1264E+04	0.2086E+01	0.2619E+09	0.2044E+09	0.2906E+09
0.7555E-02	0.2549E+06	0.1277E+04	0.2150E+01	0.2525E+09	0.1971E+09	0.2802E+09
0.7605E-02	0.2459E+06	0.1290E+04	0.2214E+01	0.2436E+09	0.1901E+09	0.2703E+09
0.7655E-02	0.2374E+06	0.1302E+04	0.2279E+01	0.2352E+09	0.1836E+09	0.2610E+09
0.7705E-02	0.2293E+06	0.1313E+04	0.2344E+01	0.2272E+09	0.1773E+09	0.2521E+09
0.7755E-02	0.2217E+06	0.1325E+04	0.2410E+01	0.2196E+09	0.1714E+09	0.2437E+09
0.7805E-02	0.2144E+06	0.1335E+04	0.2477E+01	0.2124E+09	0.1658E+09	0.2357E+09
0.7855E-02	0.2075E+06	0.1346E+04	0.2544E+01	0.2056E+09	0.1605E+09	0.2281E+09

```
0.7905E-02 0.2010E+06 0.1356E+04 0.2611E+01 0.1991E+09 0.1554E+09 0.2209E+09
0.7955E-02 0.1947E+06 0.1366E+04 0.2679E+01 0.1929E+09 0.1506E+09 0.2141E+09
0.8005E-02 0.1888E+06 0.1376E+04 0.2748E+01 0.1870E+09 0.1460E+09 0.2075E+09
0.8055E-02 0.1831E+06 0.1385E+04 0.2817E+01 0.1814E+09 0.1416E+09 0.2013E+09
0.8105E-02 0.1777E+06 0.1394E+04 0.2886E+01 0.1761E+09 0.1374E+09 0.1954E+09
0.8155E-02 0.1726E+06 0.1403E+04 0.2956E+01 0.1710E+09 0.1334E+09 0.1897E+09
0.8205E-02 0.1676E+06 0.1411E+04 0.3027E+01 0.1661E+09 0.1296E+09 0.1843E+09
0.8255E-02 0.1629E+06 0.1420E+04 0.3097E+01 0.1614E+09 0.1260E+09 0.1791E+09
0.8305E-02 0.1584E+06 0.1428E+04 0.3169E+01 0.1570E+09 0.1225E+09 0.1742E+09
0.8355E-02 0.1541E+06 0.1435E+04 0.3240E+01 0.1527E+09 0.1192E+09 0.1695E+09
0.8405E-02 0.1500E+06 0.1443E+04 0.3312E+01 0.1486E+09 0.1160E+09 0.1649E+09
0.8455E-02 0.1461E+06 0.1450E+04 0.3384E+01 0.1447E+09 0.1130E+09 0.1606E+09
0.8505E-02 0.1423E+06 0.1458E+04 0.3457E+01 0.1410E+09 0.1100E+09 0.1564E+09
0.8555E-02 0.1387E+06 0.1465E+04 0.3530E+01 0.1374E+09 0.1072E+09 0.1524E+09
0.8605E-02 0.1352E+06 0.1471E+04 0.3604E+01 0.1339E+09 0.1045E+09 0.1486E+09
0.8655E-02 0.1318E+06 0.1478E+04 0.3677E+01 0.1306E+09 0.1019E+09 0.1449E+09
0.8705E-02 0.1286E+06 0.1485E+04 0.3751E+01 0.1274E+09 0.9946E+08 0.1414E+09
0.8755E-02 0.1255E+06 0.1491E+04 0.3826E+01 0.1244E+09 0.9707E+08 0.1380E+09
0.8805E-02 0.1226E+06 0.1497E+04 0.3900E+01 0.1214E+09 0.9477E+08 0.1347E+09
0.8855E-02 0.1197E+06 0.1503E+04 0.3975E+01 0.1186E+09 0.9256E+08 0.1316E+09
0.8905E-02 0.1169E+06 0.1509E+04 0.4051E+01 0.1158E+09 0.9043E+08 0.1286E+09
0.8955E-02 0.1143E+06 0.1515E+04 0.4126E+01 0.1132E+09 0.8838E+08 0.1256E+09
0.9005E-02 0.1117E+06 0.1521E+04 0.4202E+01 0.1107E+09 0.8640E+08 0.1228E+09
0.9055E-02 0.1093E+06 0.1526E+04 0.4278E+01 0.1082E+09 0.8449E+08 0.1201E+09
0.9105E-02 0.1069E+06 0.1532E+04 0.4355E+01 0.1059E+09 0.8265E+08 0.1175E+09
0.9155E-02 0.1046E+06 0.1537E+04 0.4432E+01 0.1036E+09 0.8088E+08 0.1150E+09
0.9205E-02 0.1024E+06 0.1542E+04 0.4509E+01 0.1014E+09 0.7916E+08 0.1125E+09
 deltat t  0.925000E-02 intg t  0.925000E-02
pmaxm Pa   0.465884E+09 time at pmaxm sec   0.623000E-02
pmaxba Pa   0.363673E+09 time at pmaxba sec   0.623000E-02
pmaxbr Pa   0.516989E+09 time at pmaxbr sec   0.623000E-02
muzzle velocity m/s   0.154614E+04 time of muzzle velocity sec   0.924611E-02
total initial energy available J =   0.416340E+08
FOR PROPELLANT  1 MASS FRAC BURNT IS  0.100000E+01 AT TIME   0.690250E-02
total energy remaining in gas J=   0.253339E+08
energy loss from projectile translation J=   0.117148E+08
energy loss from projectile rotation J=   0.000000E+00
energy lost to gas and propellant motion J=   0.329245E+07
energy lost to bore resistance J=   0.000000E+00
energy lost to recoil J=   0.224172E-11
energy loss from heat transfer J=   0.129901E+07
energy lost to air resistance J=   0.000000E+00
```

INTENTIONALLY LEFT BLANK.

APPENDIX D
User's Manual

INTENTIONALLY LEFT BLANK.

IBRGA relies on an input data base consisting of all numerical parameters essential for running the code. All values are in metric units. Below is a compilation of a typical IBRGAM data base showing the name and location of each input parameter. The names for the numerical values are prefixed with an alphabetical designator corresponding to the position at which the data is tc appear, that is, from left to right. The data may be separated by blanks or commas. The units are shown to the right of each input.

A B C D E F G H I J K

record 1
- A. - chamber volume (cm^3)
- B. - groove diameter (cm)
- C. - land diameter (cm)
- D. - groove/land ratio (none)
- E. - twist (turns/caliber)
- F. - projectile travel (cm)
- G. - gradient switch (1 = Lagrange, 2 = chambrage)

record 1a (Read only if gradient switch = 2)
- A. - number of points to describe chamber (I<=10)
- B. - initial distance from breech (must be 0.0 cm)
- C. - diameter at 0 (cm)

.
.
.

Ith distance from breech (position of base of projectile (cm))
Ith diameter at Ith distance (used to calculate bore area (cm))

record 2
- A. - projectile mass (kg)
- B. - switch to calculate energy lost to air resistance
- C. - fraction of work done against bore to heat tube
- D. - gas pressure in front of projectile (Pa)

record 3
- A. - number of barrel resistance points (J<=10)
- B. - bore resistance (MPa)
- C. - travel (cm)

.
.
.

Jth bore resistance (MPa)
Jth travel (cm)

record 4

A. - mass of recoiling parts (kg)
B. - number of recoil point pairs (2)
C. - recoil force (N)
D. - recoil time (s)
E. - recoil force (N)
F. - recoil time (s)

record 5

A. - free convective heat transfer coefficient (W/cm^2-K)
B. - chamber wall thickness (cm)
C. - heat capacity of steel of chamber wall (J/g-K)
D. - initial temperature of chamber wall (K)
E. - heat loss coefficient
F. - density of chamber wall steel (g/cm^3)

record 6

A. - impetus of igniter propellant (J/g)
B. - covolume of igniter (cm^3/g)
C. - adiabatic flame temperature of igniter propellant (K)
D. - initial mass of igniter (kg)
E. - ratio of specific heats for igniter

record 7

A. - number of propellants (K<=10)

record 8

A. - switch for in-depth burning (0 none)
B. - impetus of propellant (J/g)
C. - adiabatic temperature of propellant (K)
D. - covolume of propellant (cm^3/g)
E. - initial mass of propellant (kg)
F. - density of propellant (g/cm^3)
G. - ratio of specific heats for propellant
H. - number of perforations of propellant (may be 0,1,7 ,-1 or -11 only)
(-1 for single perf outside inhibited grain,
-11 for cigarette burner)
I. - length of propellant grain (cm)
J. - diameter of inner perforations in propellant grains (cm)
K. - diameter of outer perforations of propellant grains (cm)
(used for single perforation grain)
L. - outside diameter of propellant grain (cm)
M. - distance between perf centers (cm)
N. - switch to change mass to one single perforated grain (1=yes)

record 8a (read only if in-depth burning switch is not 0)

A. - time after in-depth burning may start (msec)
B. - pressure which must be exceeded before in-depth burning may start (MPa)
C. - in-depth burning depth (mm)
D. - in-depth burning volume multiplier (m^2/m^3)

.
.
.

(Kth propellent)
A. - switch for in-depth burning (0 none)
B. - impetus of propellant (J/g)
C. - adiabatic temperature of propellant (K)
D. - covolume of propellant (cm^3/g)
E. - initial mass of propellant (kg)
F. - density of propellant (g/cm^3)
G. - ratio of specific heats for propellant
H. - number of perforations of propellant (may be 0,1,7, -1 or -11 only)
(-1 for single perf outside inhibited grain,
-11 for cigarette burner)
I. - length of propellant grain (cm)
J. - diameter of inner perforations in propellant grains (cm)
K. - diameter of outer perforations of propellant grains (cm)
(used for single perforation grain)
L. - outside diameter of propellant grain (cm)
M. - distance between perf centers (cm)
N. - switch to change mass to one single perforated grain (1=yes)

record 8k (read only if in-depth burning switch is not 0)
A. - time after in-depth burning may start (msec)
B. - pressure which must be exceeded before in-depth burning may start (MPa)
C. - in-depth burning depth (mm)
D. - in-depth burning volume multiplier (m^2/m^3)
.
.

record 9
A. - number of surface burning rate points (J<=10) for propellent 1
B. - exponent
C. - coefficient (cm/s MPa^{ai})
D. - pressure (MPa)
.
.
.

Jth exponent
Jth coefficient
Jth pressure
.

record 9a (Read only if in-depth burning switch is not 0)
A. number of in-depth burning surface area burning rate points (M<=10) for propellant 1
B. exponent
C. coefficient (cm/s MPa^{ai})
D. pressure (MPa)
.
.

Mth exponent
Mth coefficient
Mth pressure

.
.
.

A. - number of surface burning rate points (L<=10) for propellent K
B. - exponent
C. - coefficient (cm/s MPa^{ai})
D. - pressure (MPa)

.
.
.

Lth exponent
Lth coefficient
Lth pressure

record 9a (Read only if in-depth burning switch is not 0)

A. number of in-depth burning surface area burning rate points (N<=10) for propellant K
B. exponent
C. coefficient (cm/s MPa^{ai})
D. pressure (MPa)

.
.
Nth exponent
Nth coefficient
Nth pressure
.
.

record 10

A. - time increment (ms)
B. - print increment (ms)
C. - time to stop calculation (ms)

No of Copies	Organization
(Unclass., unlimited) 12	Administrator
(Unclass., limited) 2	Defense Technical Info Center
(Classified) 2	ATTN: DTIC-DDA
	Cameron Station
	Alexandria, VA 22304-6145
1	HQDA (SARD-TR)
	WASH DC 20310-0001
1	Commander
	US Army Materiel Command
	ATTN: AMCDRA-ST
	5001 Eisenhower Avenue
	Alexandria, VA 22333-0001
1	Commander
	US Army Laboratory Command
	ATTN: AMSLC-DL
	Adelphi, MD 20783-1145
2	Commander
	Armament RD&E Center
	US Army AMCCOM
	ATTN: SMCAR-MSI
	Picatinny Arsenal, NJ 07806-5000
2	Commander
	Armament RD&E Center
	US Army AMCCOM
	ATTN: SMCAR-TDC
	Picatinny Arsenal, NJ 07806-5000
1	Director
	Benet Weapons Laboratory
	Armament RD&E Center
	US Army AMCCOM
	ATTN: SMCAR-LCB-TL
	Watervliet, NY 12189-4050
1	Commander
	US Army Armament, Munitions and Chemical Command
	ATTN: SMCAR-ESP-L
	Rock Island, IL 61299-5000
1	Commander
	US Army Aviation Systems Command
	ATTN: AMSAV-DACL
	4300 Goodfellow Blvd.
	St. Louis, MO 63120-1798
1	Director
	US Army Aviation Research and Technology Activity
	Ames Research Center
	Moffett Field, CA 94035-1099

No of Copies	Organization
1	Commander
	US Army Missile Command
	ATTN: AMSMI-RD-CS-R (DOC)
	Redstone Arsenal, AL 35898-5010
1	Commander
	US Army Tank Automotive Command
	ATTN: AMSTA-TSL (Technical Library)
	Warren, MI 48397-5000
1	Director
	US Army TRADOC Analysis Command
	ATTN: ATAA-SL
	White Sands Missile Range, NM 88002-5502
(Class. only) 1	Commandant
	US Army Infantry School
	ATTN: ATSH-CD (Security Mgr.)
	Fort Benning, GA 31905-5660
(Unclass. only) 1	Commandant
	US Army Infantry School
	ATTN: ATSH-CD-CSO-OR
	Fort Benning, GA 31905-5660
(Class. only) 1	The Rand Corporation
	P.O. Box 2138
	Santa Monica, CA 90401-2138
1	Air Force Armament Laboratory
	ATTN: AFATL/DLODL
	Eglin AFB, FL 32542-5000

Aberdeen Proving Ground

Dir, USAMSAA
ATTN: AMXSY-D
AMXSY-MP, H. Cohen

Cdr, USATECOM
ATTN: AMSTE-TO-F

Cdr, CRDEC, AMCCOM
ATTN: SMCCR-RSP-A
SMCCR-MU
SMCCR-MSI

Dir, VLAMO
ATTN: AMSLC-VL-D

No. of Copies	Organization
1	Commander USA Concepts Analysis Agency ATTN: D. Hardison 8120 Woodmont Avenue Bethesada, MD 20014-2797
1	HQDA/DAMA-ZA Washington, DC 20310-2500
1	HQDA/DAMA-CSM Washington, DC 20310-2500
1	C.I.A. 01R/DB/Standard GE47 HQ Washington, DC 20505
1	US Army Ballistic Missile Defense Systems Command Advanced Technology Center P.O. Box 1500 Huntsville, AL 35807-3801
1	Chairman DOD Explosives Safety Board Room 856-C Hoffman Bldg 1 2461 Eisenhower Avenue Alexandria, VA 22331-9999
1	Commander US Army Materiel Command ATTN: AMCPM-GCM-WF 5001 Eisenhower Avenue Alexandria, VA 22333-50001
1	Commander US Army Materiel Command ATTN: AMCDE-DW 5001 Eisenhower Avenue Alexandria, VA 22333-5001
5	Project Manager Cannon Artillery Weapons Systems, ARDEC AMCCOM ATTN: AMCPM-CW AMCPM-CWW AMCPM-CWS/M. Fisette AMCPM-CWA/H. Haussman AMCPM-CWA-S/ R. DeKleine Picatinny Arsenal, NJ 07806-5000
2	Project Manager Munitions Production Base Modernization and Expansion ATTN: AMCPM-PBM/A. Siklosi AMCPM-PBM-E/L. Laibson Picatinny Arsenal, NJ 07806-5000
3	Project Manager Tank Main Armament System ATTN: AMCPM-TMA/K. Russell AMCPM-TMA-105 AMCPM-TMA-120 Picatinny Arsenal, NJ 07806-5000
1	HQDA DAMA-ART-M Washington, DC 20310-2500
1	Commander US Army ARDEC ATTN: SMCAR-LC/ LTC N. Barron Picatinny Arsenal, NJ 07806-5000
7	Commander US Army ARDEC ATTN: SMCAR-LCA/ A. Beardell D. Downs S. Einstein S. Westley S. Bernstein C. Roller J. Rutkowski Picatinny Arsenal, NJ 07806-5000
3	Commander US Army ARDEC ATTN: SMCAR-LCB-I/ D. Spring SMCAR-LCE SMCAR-LCM-E/ S. Kaplowitz Picatinny Arsenal, NJ 07806-5000

No. of Copies	Organization
4	Commander US Army ARDEC ATTN: SMCAR-LCS SMCAR-LCU-CT/ E. Barrieres R. Davitt SMCAR-LCU-CV/ C. Mandala Picatinny Arsenal, NJ 07806-5000
3	Commander US Army ARDEC ATTN: SMCAR-LCW-A/ M. Salsbury SMCAR-SCA/ L. Stiefel B. Brodman Picatinny Arsenal, NJ 07806-5000
1	Director US Army Aviation Research and Technology Activity Ames Research Center Moffett Field, CA 04035-1099
1	Commander CECOM R&D Technical Library ATTN: ASNC-ELC-T (Report Section) Fort Monmouth, NJ 07703-5001
1	Commander US Army Harry Diamond Laboratory ATTN: DELHD-TA-L 2800 Powder Mill Rd. Adelphi, MD 20783-1145

No. of Copies	Organization
1	Commandant US Army Aviation School ATTN: Aviation Agency Fort Rucker, AL 36360
1	Project Manager US Army Tank Automotive Command Improved TOW Vehicle ATTN: AMCPM-ITV Warren, MI 48397-5000
2	Program Manager M1 Abrams Tank System ATTN: AMCPM-GMC-SA/ T. Dean Warren, MI 48092-2498
1	Project Manager Fighting Vehicle Systems ATTN: AMCPM-FVS Warren, MI 48092-2498
1	President US Army Armor & Engineer Board ATTN: ATZK-AD-S Fort Knox, KY 40121-5200
1	Project Manager M-60 Tank Development ATTN: AMCPM-M60TD Warren, MI 48092-2498
1	Commander US Army Training & Doctrine Command ATTN: ATCD-MA/MAJ Williams Fort Monroe, VA 23651
2	Commander US Army Materials and Mechanics Research Center ATTN: AMXMR-ATL Watertown, MA 02172
1	Commander US Army Research Office ATTN: Tech Library P.O. Box 12211 Research Triangle Park, NC 27709-2211

No. of Copies	Organization
1	Commander US Army Belvoir Research and Development Center ATTN: STRBE-WC Fort Belvoir, VA 22060-5606
1	Commander US Army Logistics Mgmt Ctr Defense Logistics Studies Fort Lee, VA 23801
1	Commandant US Army Command and General Staff College Fort Leavenworth, KS 66027
1	Commandant US Army Special Warfare School ATTN: Rev & Tng Lit Div Fort Bragg, NC 28307
3	Commander Radford Army Ammunition Plant ATTN: SMCAR-QA/HI LIB Radford, VA 24141-0298
1	Commander US Army Foreign Science & Technology Center ATTN: AMXST-MC-3 220 Seventh Street, NE Charlottesville, VA 22901-5396
2	Commander Naval Sea Systems Command ATTN: SEA 62R SEA 64 Washington, DC 20362-5101
1	Commander Naval Air Systems Command ATTN: AIR-954-Tech Lib Washington, DC 20360
1	Assistant Secretary of the Navy (R,E, and S) ATTN: R. Reichenbach Room 5E787 Pentagon Bldg Washington, DC 20375
1	Naval Research Laboratory Tech Library Washington, DC 20375
2	Commandant US Army Field Artillery Center & School ATTN: ATSF-CO-MW/B. Willis Ft. Sill, OK 73503-5600
1	Office of Naval Research ATTN: Code 473, R.S. Miller 800 N. Quincy Street Arlington, VA 22217-9999
3	Commandant US Army Armor School ATTN: ATZK-CD-MS/ M. Falkovitch Armor Agency Fort Knox, KY 40121-5215
2	Commander US Naval Surface Weapons Center ATTN: J.P. Consaga C. Gotzmer Indian Head, MD 20640-5000
4	Commander Naval Surface Weapons Center ATTN: Code 240/S. Jacobs Code 730 Code R-13/K. Kim R. Bernecker Silver Spring, MD 20903-5000

No. of Copies	Organization
2	Commanding Officer Naval Underwater Systems Center ATTN: Code 5B331/R.S. Lazar Tech Lib Newport, RI 02840
5	Commander Naval Surface Weapons Center ATTN: Code G33/J.L. East W. Burrell J. Johndrow Code G23/D. McClure Code DX-21 Tech Lib Dahlgren, VA 22448-5000
3	Commander Naval Weapons Center ATTN: Code 388/C.F. Price T. Parr Info Sci Div China Lake, CA 9355-6001
2	Superintendent Naval Postgraduate School Dept. of Mech. Engineering Monterey, CA 93943-5100
1	Program Manager AFOSR Directorate of Aerospace Sciences ATTN: L.H. Caveny Bolling AFB, DC 20332-0001
6	Commander Naval Ordnance Station ATTN: P.L. Stang L. Torreyson T.C. Smith D. Brooks W. Vienna Tech Library Indian Head, MD 20640-5000
1	AF Astronautics Laboratory AFAL/TSTL (Technical Library) Edwards AFB, CA 93523-5000
1	AFSC/SDOA Andrews AFB, MD 20334
1	AFATL/DLYV Eglin AFB, FL 32542-5000
1	AFATL/DLXP Eglin AFB, FL 32542-5000
1	AFATL/DLJE Eglin AFB, FL 32542-5000
1	NASA/Lyndon B. Johnson Space Center ATTN: NHS-22 Library Section Houstin, TX 77054
1	AFELM, The Rand Corporation ATTN: Library D 1700 Main Street Santa Monica, CA 90401-3297
3	AAI Corporation ATTN: J. Herbert J. Frankle D. Cleveland P.O. Box 126 Hunt Valley, MD 21030-0126
1	Aerojet Ordnance Company ATTN: D. Thatcher 2521 Michelle Drive Tustin, CA 92680-7014
1	Aerojet Solid Propulsion Co. ATTN: P. Micheli Sacramento, CA 95813
1	Atlantic Research Corporation ATTN: M. King 5390 Cherokee Avenue Alexandria, VA 22312-2302
3	AFRPL/DY, Stop 24 ATTN: J. Levine/DYCR R. Corley/DYC D. Williams/DYCC Edwards AFB, CA 93523-5000

No. of Copies	Organization
1	AVCO Everett Research Laboratory ATTN: D. Stickler 2385 Revere Beach Parkway Everett, MA 02149-5936
2	Calspan Corporation ATTN: C. Murphy P.0. Box 400 Buffalo, NY 14225-0400
1	General Electric Company Armament Systems Dept. ATTN: M.J. Bulman 128 Lakeside Avenue Burlington, VT 05401-4985
1	IITRI ATTN: M.J. Klein 10 W. 35th Street Chicago, IL 60616-3799
1	Hercules Inc. Allegheny Ballistics Laboratory ATTN: R.B. Miller P.O. Box 210 Cumberland, MD 21501-0210
1	Hercules Inc. Bacchus Works ATTN: K.P. McCarty P.O. Box 98 Magna, UT 84044-0098
1	Hercules Inc. Radford Army Ammunition Plant ATTN: J. Pierce Radford, VA 24141-0299
2	Lawrence Livermore National Laboratory ATTN: L-355/ A. Buckingham M. Finger P.O. Box 808 Livermore, CA 94550-0622
1	Lawrence Livermore National Laboratory ATTN: L-324/M. Constantino P.O. Box 808 Livermore, CA 94550-0622
1	Olin Corporation Badger Army Ammunition Plant Baraboo, WI 53913
1	Olin Corporation Smokeless Powder Operations ATTN: D.C. Mann P.O. Box 222 St. Marks, FL 32355-0222
1	Paul Gough Associates, Inc. ATTN: P.S. Gough P.O. Box 1614 1048 South St. Portsmouth, NH 03801-1614
1	Physics International Company ATTN: Library/H. Wayne Wampler 2700 Merced Street San Leandro, CA 984577-5602
1	Princeton Combustion Research Laboratory, Inc. ATTN: M. Summerfield 475 US Highway One Monmouth Junction, NJ 08852-9650
2	Rockwell International Rocketdyne Division ATTN: BA08/J.E. Flanagan J. Gray 6633 Canoga Avenue Canoga Park, CA 91303-2703
3	Thiokol Corporation Huntsville Division ATTN: D. Flanigan R. Glick Tech Library Huntsville, AL 35807

No. of Copies	Organization
2	Thiokol Corporation Elkton Division ATTN: R. Biddle Tech Library P.O. Box 241 Elkton, MD 21921-0241
1	Veritay Technology, Inc. ATTN: E. Fisher 4845 Millersport Hwy. P.O. Box 305 East Amherst, NY 14501-0305
1	Universal Propulsion Company ATTN: H.J. McSpadden Black Canyon Stage 1 Box 1140 Phoenix, AZ 85029
1	Battelle Memorial Institute ATTN: Tech Library 505 King Avenue Columbus, OH 43201-2693
1	Brigham Young University Dept. of Chemical Engineering ATTN: M. Beckstead Provo, UT 84601
1	California Institute of Tech 204 Karman Lab Main Stop 301-46 ATTN: F.E.C. Culick 1201 E. California Street Pasadena, CA 91109
1	California Institute of Tech Jet Propulsion Laboratory ATTN: L.D. Strand 4800 Oak Grove Drive Pasadena, CA 91109-8099
1	University of Illinois Dept of Mech/Indust Engr ATTN: H. Krier 144 MEB; 1206 N. Green St. Urbana, IL 61801-2978
1	University of Massachusetts Dept of Mech Engineering ATTN: K. Jakus Amherst, MA 01002-0014
1	University of Minnesota Dept of Mech Engineering ATTN: E. Fletcher Minneapolis, MN 55414-3368
1	Case Western Reserve University Division of Aerospace Sciences ATTN: J. Tien Cleveland, OH 44135
3	Georgia Institute of Tech School of Aerospace Eng ATTN: B.T. Zinn E. Price W.C. Strahle Atlanta, GA 30332
1	Institute of Gas Technology ATTN: D. Gidaspow 3424 S. State Street Chicago, II 60616-3896
1	Johns Hopkins University Applied Physics Laboratory Chemical Propulsion Information Agency ATTN: T. Christian Johns Hopkins Road Laurel, MD 20707-0690
1	Massachusetts Institute of Technology Dept of Mechanical Engineering ATTN: T. Toong 77 Massachusetts Avenue Cambridge, MA 02139-4307
1	Pennsylvania State University Applied Research Laboratory ATTN: G.M. Faeth University Park, PA 16802-7501

No. of Copies	Organization
1	Pennsylvania State University Dept of Mech Engineering ATTN: K. Kuo University Park, PA 16802-7501
1	Purdue University School of Mechanical Engineering ATTN: J.R. Osborn TSPC Chaffee Hall West Lafayette, IN 47907-1199
1	SRI International Propulsion Sciences Division ATTN: Tech Library 333 Ravenswood Avenue Menlo Park, CA 94025-3493
1	Rensselaer Ploytechnic Inst. Department of Mathematics Troy, NY 12181
2	Director Los Alamos Scientific Lab ATTN: T3/D. Butler M. Division/B. Craig P.O. Box 1663 Los Alamos, NM 87544
1	General Applied Sciences Lab ATTN: J. Erdos 77 Raynor Ave. Ronkonkama, NY 11779-6649
1	Battelle PNL ATTN: Mr. Mark Garnich P.O. Box 999 Richland, WA 99352
1	Stevens Institute of Technology Davidson Laboratory ATTN: R. McAlevy, III Castle Point Station Hoboken, NJ 07030-5907

No. of Copies	Organization
1	Rutgers University Dept of Mechanical and Aerospace Engineering ATTN: S. Temkin University Heights Campus New Brunswick, NJ 08903
1	University of Southern California Mechanical Engineering Dept. ATTN: 0HE200/M. Gerstein Los Angeles, CA 90089-5199
2	University of Utah Dept. of Chemical Engineering ATTN: A. Baer G. Flandro Salt Lake City, UT 84112-1194
1	Washington State University Dept of Mech Engineering ATTN: C.T. Crowe Pullman, WA 99163-5201
1	Honeywell Inc. ATTN: R.E. Tompkins MN38-3300 10400 Yellow Circle Drive Minnetonka, MN 55343
1	Science Applications, Inc. ATTN: R.B. Edelman 23146 Cumorah Crest Drive Woodland Hills, CA 91364-3710
	Aberdeen Proving Ground
	Cdr, CSTA ATTN: STECS-LI/R. Hendricksen

USER EVALUATION SHEET/CHANGE OF ADDRESS

This laboratory undertakes a continuing effort to improve the quality of the reports it publishes. Your comments/answers below will aid us in our efforts.

1. Does this report satisfy a need? (Comment on purpose, related project, or other area of interest for which the report will be used.) _____

2. How, specifically, is the report being used? (Information source, design data, procedure, source of ideas, etc.) _____

3. Has the information in this report led to any quantitative savings as far as man-hours or dollars saved, operating costs avoided, or efficiencies achieved, etc? If so, please elaborate. _____

4. General Comments. What do you think should be changed to improve future reports? (Indicate changes to organization, technical content, format, etc.) _____

BRL Report Number _____ Division Symbol _____

Check here if desire to be removed from distribution list. ____

Check here for address change. ____

Current address: Organization _____
Address _____

----------FOLD AND TAPE CLOSED----------

Director
U.S. Army Ballistic Research Laboratory
ATTN: SLCBR-DD-T
Aberdeen Proving Ground, MD 21005-5066

OFFICIAL BUSINESS

NO POSTAGE NECESSARY IF MAILED IN THE UNITED STATES

BUSINESS REPLY LABEL
FIRST CLASS PERMIT NO. 12062 WASHINGTON D.C.

POSTAGE WILL BE PAID BY DEPARTMENT OF THE ARMY

Director
U.S. Army Ballistic Research Laboratory
ATTN: SLCBR-DD-T
Aberdeen Proving Ground, MD 21005-9989